DECEMBER 2018, NO 9

Scripta-Ingenia

Números reais imaginados

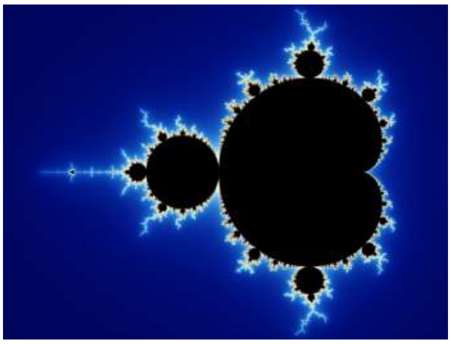

Conjunto de Mandelbrot (fonte: Wikipedia)

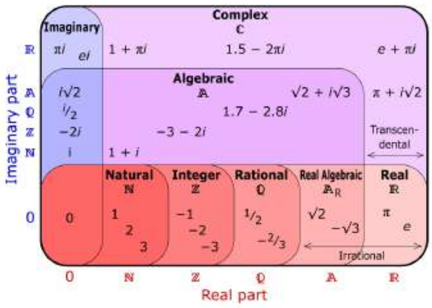

Representação esquemática ilustrada da inclusão dos sistemas numéricos (fonte: thinkzone.wlonk.com)

Muito se fala de números. Aqui e ali sempre aparecem quando menos se espera. Sejam eles naturais, inteiros, racionais, reais ou complexos. Usando os números naturais como base, os quais servem para contar, obtêm-se depois por construção os números inteiros e os racionais. Os números reais aparecem também por um processo construtivo e estudam-se todas as suas propriedades e interacções — todas, até à exaustão! No quadro da figura ao lado podemos ver como a construção dos sistemas numéricos, que começa por isso com os números naturais, e que depois se extende, por sucessivas construções, até aos números reais e complexos.

Os números naturais com as operações de adição e multiplicação formam um sistema algébrico designado por semi-anel. Os números inteiros surgem da necessidade de resolver equações da forma $x + a = b$ cuja solução queremos representar por $x = b - a$. Os números racionais sugem da necessidade de resolver as equações da forma $ax = b$, sempre que $a \neq 0$, cuja solução queremos representar por $x = \frac{b}{a}$. A passagem dos racionais para os reais é mais delicada e tem a ver com a necessidade de calcular limites de certas sucessões de números racionais. Admitindo que os números reais são a conceptualização formal de um conceito bastante real tal como os pontos sobre uma reta geométrica, chegamos naturalmente aos números complexos como os pontos sobre um plano, ou seja, são pares de numeros reais constituindo um número (complexo) que se caracteriza por ter uma componente real e outra imaginária. O conjunto de Mandelbrot é um bonito exemplo de um conjunto de pontos, aos quais chamamos números, mas serão eles reais ou apenas imaginados?

Ficha Técnica
Director: Nelson Martins Ferreira
Proprietário: Instituto Politécnico de Leiria, anotado na ERC
Morada: Rua General Norton de Matos; Apartado 4133; 2411-901 Leiria, Portugal
Director Adjunto: Nuno Alves; Sub Director: Artur Mateus
Editor: Nelson Martins Ferreira; Sede de Redação: Rua General Norton de Matos; Apartado 4133; 2411-901 Leiria, Portugal; Contacto: scripta.ingenia@ipleiria.pt
Colaboradores e estatuto editorial: `http://cdrsp.ipleiria.pt/scriptaingenia/`

A Scripta-Ingenia assume-se como uma revista de divulgação científica tratando temas da ciência e da tecnologia, cobrindo todas as áreas do saber no domínio das ciências exactas ou aplicadas. Interessa-se ainda por artigos de opinião, sobre tópicos científicos ou não, desde que escritos por autores na área das ciências e da engenharia, e que reflitam as suas opiniões enquanto membros dessa comunidade.

Director and Chief Editor — Nelson Martins-Ferreira
CDRSP-ESTG, IPLeiria

I cannot help feeling there is something essentially wrong about love. Friends may quarrel or drift apart, close relations too, but there is not this pang, this pathos, this fatality which clings to love. Friendship never has that doomed look. Why, what is the matter? I have not stopped loving you, but because I cannot go on kissing your dim dear face, we must part, we must part. Why is this so? What is this mysterious exclusiveness? One may have a thousand friends, but only one love-mate. Harems have nothing to do with this matter: I am speaking of dance, not gymnastics. Or can one imagine a tremendous Turk loving every one of his four hundred wives as I love you? For if I say 'two' I have started to count and there is no end to it. There is only one real number: One. And love, apparently, is the best exponent of this singularity.

Vladimir Nabokov, The Real Life of Sebastian Knight

Rotating Magnetic Solutions for 2+1D Einstein Maxwell Chern-Simons

by P. CASTELO FERREIRA

Centre for Rapid and Sustainable Product Development
Polytechnic Institute of Leiria
Author email: pedro.castelo.ferreira@gmail.com

Abstract In this article are computed magnetic solutions of Einstein Maxwell Chern-Simons theory coupled to a dilaton-like scalar field. These solutions are computed by applying a space-time duality suggested by the author to known electric solutions of the same theory. As a redundancy check for the space-time duality it is explicitly shown that the magnetic configurations obtained are, as expected, solutions of the equations of motion. The magnetic configurations have metric determinant $\sqrt{-g} \sim r^p$ for the range of the parameter $p \in]-\infty, +\infty[/\{-1\}$ and are interpreted either as magnetic string-like configurations, configurations driven by an externally applied magnetic field or cosmological-like solutions with background magnetic fields.

1 Introduction

The first studies on classical gravitational solutions in $2+1$-dimensional space-times date back to 1984 and addressed Cosmological Einstein theories [1, 2]. Later developments addressed neutral solutions for Einstein theory (AdS BTZ black-hole) [3], Einstein Chern-Simons theory [4, 5] and the rotating BTZ black-hole [6, 7]. Following these developments charged solutions were studied for Einstein Maxwell Chern-Simons theory [8, 9, 10, 11, 12], Einstein Maxwell theory [13, 14], Dilaton Einstein Maxwell theories [15, 16, 17, 18, 19, 20, 21, 22] and electric solutions of Einstein Maxwell Chern-Simons theory with a scalar field [23], as well as for Chern-Simons gravity [24, 25, 26, 27, 28, 29, 30].

In this article are computed new magnetic solutions that further extend the known existing solutions for Einstein Maxwell Chern-Simons theory coupled to a Dilaton-like scalar field. As a motivation for the several fields and sectors of the full theory studied here it is relevant to note that, when considering $2+1$-dimensional gravitational solutions the inclusion of a scalar field is a natural extension of Einstein theory and it is justified by noting that a dimensional reduction from $3+1$-dimensions generates such a scalar field, whether it is a Dilaton field [15, 16, 31] or obtained by gauging a higher dimensional symmetry [32, 33]. In addition when considering electromagnetic field solutions in $2+1$-dimensions the Chern-Simons term [34, 35] is also a natural extension of Maxwell theory, at quantum level only the Maxwell Chern-Simons theory is consistent such that the Chern-Simons term is a quantum correction of the Maxwell theory [36, 37, 38, 39].

As possible physical frameworks were such solutions may be relevant we note that $2+1$-dimensional theories are often considered simpler laboratories for higher dimensional theories [7], higher dimensional examples with similar frameworks to the one discussed here are: inflationary models with exponential potentials [40]; domain walls in 4+1-dimensions [41]; and cosmological solutions in 4+1-dimensions [42, 43]. In addition often $3+1$-dimensional systems exhibiting cylindrical symmetry are considered as effective $2+1$-dimensional systems [32, 33, 44] as it is the example of cylindrical gravitational waves [45, 46, 47, 48, 49].

To compute these new solutions it is applied the space-time suggested by the author in [50] to the previously computed electric solutions for this theory [23]. These dualities constitutes a generalization of a duality previously suggested in [4]. Shortly resuming the results obtained in [50], starting from a specific metric parameterization and Maxwell Chern-Simons Lagrangian

$$\begin{aligned} ds^2 &= -f^2 dt^2 + dr^2 + h^2 (d\varphi + A dt)^2 \ , \\ \mathcal{L}^{\rm MCS} &= F \wedge *F + m\, A \wedge F \ , \end{aligned} \tag{1.1}$$

with the standard electric and magnetic field definitions

$$\begin{aligned} E_* &= F_{tr} = \partial_t A_r - \partial_r A_t \ , \\ B_* &= F_{r\varphi} = \partial_r A_\varphi - \partial_\varphi A_r \ , \end{aligned} \tag{1.2}$$

where stared fields E_* and B_* stand for the electromagnetic fields in a specific coordinate frame while non stared field E and B stand for the fields in the Cartan-frame (details are given in appendix A), there are three possible dualities that map electric into magnetic solutions. Specifically the interchange between time and angular variable corresponding to the two distinct duality maps

$$\left\{ \begin{array}{lcl} t & \to & i\varphi \\ \varphi & \to & it \end{array} \right. \Rightarrow \left\{ \begin{array}{lcl} f & \to & ih \\ h & \to & if \end{array} \right. , \left\{ \begin{array}{lcl} E_* & \to & -iB_* \\ B_* & \to & -iE_* \ , \end{array} \right. \tag{1.3}$$

and

$$\left\{\begin{array}{lcl} t & \to & \varphi \\ \varphi & \to & t \end{array}\right. \Rightarrow \left\{\begin{array}{lcl} f & \to & h \\ h & \to & f \end{array}\right. , \left\{\begin{array}{lcl} E_* & \to & -B_* \\ B_* & \to & -E_* \, . \end{array}\right. \tag{1.4}$$

A third duality map relates both the duality maps (1.3) and (1.4) by a double Wick rotation

$$\left\{\begin{array}{lcl} t & \to & it \\ \varphi & \to & i\varphi \end{array}\right. \Rightarrow \left\{\begin{array}{lcl} f & \to & if \\ h & \to & ih \end{array}\right. , \left\{\begin{array}{lcl} E_* & \to & iE_* \\ B_* & \to & iB_* \, . \end{array}\right. \tag{1.5}$$

This work is organized as follows, in section 2 the space-time dualities are applied to the electric gravitational solutions computed in [23] which are in this way mapped into new magnetic gravitational solutions. Are also analyzed the singularities, curvature, horizons, mass, angular momentum and magnetic flux for these magnetic configurations. In section 3 are summarized and discussed the results obtained, in particular are interpreted either as magnetic string-like solutions, configurations driven by an external magnetic field or cosmological-like solutions. In addition in appendix A are re-derived directly from the equations of motion in the Cartan-frame the solutions discussed in section 2 and in appendix B are listed, for particular cases not included in the main text, the expressions for the mass, angular momentum and magnetic flux of the magnetic configurations.

2 Magnetic solutions for Minkowski space-time

In this section we derive explicit magnetic solutions for Einstein Maxwell Chern-Simons coupled to a scalar field employing the space-time duality developed in the previous section applied to the electric solutions computed in [23]. Hence we are considering the same Action of [23] that explicitly written in tensor notation is

$$\begin{aligned} S = \ & \frac{1}{2\pi}\int_M d^3x \left\{ \sqrt{-\tilde{g}} \left[e^{a\phi}\left(\tilde{R} + 2\lambda(\partial\phi)^2\right) - e^{b\phi}\Lambda \right.\right. \\ & \left.\left. + \hat{\epsilon}\frac{e^{c\phi}}{2}\,\tilde{F}_{\mu\nu}\tilde{F}^{\mu\nu}\right] - \hat{\epsilon}\frac{m}{2}\,\epsilon^{\mu\nu\lambda}\tilde{A}_\mu\tilde{F}_{\nu\lambda}\right\} , \end{aligned} \tag{2.1}$$

where $\hat{\epsilon} = \pm 1$ sets the relative sign between the gauge and gravitational sector and the remaining terms follow the conventions of [23] such that the metric has Minkowski ADM signature $\mathrm{diag}(-,+,+)$ and we are employing natural units $c_{\rm light} = \hbar = 1$. We recall that $\hat{\epsilon} = +1$ stands for a ghost gauge sector such that the gauge fields contribution to the total energy is negative while $\hat{\epsilon} = -1$ stands for a standard gauge sector such that the gauge fields contribution to the total energy is positive [51, 23, 50].

2.1 Obtaining the solutions employing space-time duality

Directly applying the duality map (1.3) to the electric solutions studied in [23] accounts for mapping the metric parameterization and Maxwell Chern-Simons (1.1) into

$$\begin{aligned} d\tilde{s}^2 &= -\tilde{f}^2(dt + \tilde{A}d\varphi)^2 + dr^2 + \tilde{h}^2 d\varphi^2 \, , \\ \tilde{\mathcal{L}}^{\rm MCS} &= -\tilde{F}\wedge *\tilde{F} - m\tilde{A}\wedge\tilde{F} \, , \end{aligned} \tag{2.2}$$

which is equivalent to the metric components map

$$\left\{\begin{array}{lcl} \tilde{g}_{00} & = & -f^2 + h^2A^2 \\ \tilde{g}_{11} & = & 1 \\ \tilde{g}_{22} & = & h^2 \\ \tilde{g}_{02} & = & h^2 A \end{array}\right. , \left\{\begin{array}{lcl} \tilde{g}_{00} & = & -\tilde{f}^2 \\ \tilde{g}_{11} & = & 1 \\ \tilde{g}_{22} & = & \tilde{h}^2 - \tilde{f}^2\tilde{A}^2 \\ \tilde{g}_{02} & = & -\tilde{f}^2\tilde{A} \end{array}\right. , \tag{2.3}$$

and the field components map

$$\begin{aligned} &\left\{\begin{array}{lcl} f^2 & = & \dfrac{\tilde{f}^2\,\tilde{h}^2}{\tilde{h}^2 - \tilde{f}^2\,\tilde{A}^2} \\ h^2 & = & \tilde{h}^2 - \tilde{f}^2\,\tilde{A}^2 \\ A & = & -\dfrac{\tilde{A}\,\tilde{f}^2}{\tilde{h}^2 - \tilde{f}^2\,\tilde{A}^2} \end{array}\right. , \\ &\left\{\begin{array}{lcl} E_* & = & i\tilde{B}_*\left(\tilde{f} = f, \tilde{h} = h\right) \\ B_* & = & i\tilde{E}_*\left(\tilde{f} = f, \tilde{h} = h\right) \end{array}\right. . \end{aligned} \tag{2.4}$$

Hence the magnetic solutions for the action (2.1) with $a = 0$, $c = -b/2$ and $\lambda \neq b^2/8$ [23]

$$\begin{aligned} \phi &= -\frac{2}{b}\ln(C_\phi\, r) \\ \tilde{f} &= C_f\sqrt{r} \\ \tilde{h} &= C_h\, r^{p-\frac{1}{2}} \\ \tilde{A} &= C_A\, r^{p-1} + \theta \\ \tilde{B}_* &= C_B\, r^{p-2} \\ \tilde{A}_\varphi &= \frac{C_B}{p-1}\, r^{p-1} \end{aligned} \tag{2.5}$$

where C_h, C_f, b and θ are free parameters and the constants λ, C_ϕ, C_A and C_B have the following allowed values

$$\begin{aligned}
\lambda &= -\frac{b^2}{8}p\,,\\
C_\phi &= |m|\sqrt{\frac{1-6x}{1-3p}}\,,\\
C_A &= \frac{\mathrm{sign}\,(m)\,C_h}{C_f(1-p)}\sqrt{\frac{1-3p}{1-6x}}\,,\\
C_B &= \frac{C_h}{\sqrt{2|m|}}\sqrt{\frac{\hat\epsilon(p-4x+6px)}{1-3p}}\left(\frac{1-3p}{1-6x}\right)^{\frac{3}{4}}\,,
\end{aligned} \tag{2.6}$$

expressed in terms of a numerical parameter $p = p(x)$ and the ratio of the cosmological constant Λ to the topological mass squared m^2

$$x = \frac{\Lambda}{m^2}\,. \tag{2.7}$$

In the above expression for C_B the factor of $(1-3p)$ was not simplified in order to maintain the factor inside of the square root explicitly positive. For completeness the equations of motion in the Cartan-frame for this metric parameterization are also solved in Appendix A.

Imposing reality conditions for the solution constants there are four distinct allowed solutions depending on the parameter $\hat\epsilon = \pm 1$, the range of values for the ratio x and the respective bounds on the parameter p

$$\begin{array}{lll}
\text{I.} & \hat\epsilon = +1\,, & x \in \left]0, \tfrac{1}{2}\right]\,,\\
& & p = -\frac{3x-\sqrt{x(2-3x)}}{1-6x} \in \left]0,\tfrac{1}{2}\right]\\
\text{II.} & \hat\epsilon = -1\,, & x \in \left]0, \tfrac{1}{6}\right[\,\cup\, \left[\tfrac{1}{2},\tfrac{2}{3}\right]\,,\\
& & p = -\frac{3x-\sqrt{x(2-3x)}}{1-6x} \in \left]0,\tfrac{1}{3}\right[\,\cup\, \left[\tfrac{1}{2},\tfrac{2}{3}\right]\\
\text{III.} & \hat\epsilon = +1\,, & x \in \left]0, \tfrac{1}{6}\right[/ \left\{\tfrac{1}{14}\right\}\,,\\
& & p = -\frac{3x+\sqrt{x(2-3x)}}{1-6x} \in \left]-\infty,0\right[/\{-1\}\\
\text{IV.} & \hat\epsilon = -1\,, & x \in \left]\tfrac{1}{6}, \tfrac{2}{3}\right]\,,\\
& & p = -\frac{3x+\sqrt{x(2-3x)}}{1-6x} \in \left[\tfrac{2}{3},+\infty\right[\,.
\end{array} \tag{2.8}$$

The particular case $x = p = 0$ corresponds to $\lambda = 0$ and allows both for a limiting solution with $\tilde B_* = 0$, $m \neq 0$, $\phi \neq 0$ (a non-trivial dilaton field) and the trivial solution with $m = \Lambda = \phi = \tilde B_* = 0$ corresponding to empty flat Minkowski space-time. We note that the value of the cosmological constant is constrained by the mass $\Lambda < m^2$ (A.34) such that either of the limits $\Lambda \to 0$ or $m \to 0$ are equivalent to the limit $x \to 0$. In the following we consider that the particular case $x \to 0$ is retrieved by taking the limit $m \to 0$ such that this limiting solution corresponds to the trivial solution, empty flat Minkowski space-time. In solution I, the particular case $x = 1/6$ is well defined corresponding to the same solutions (2.5) with $p = 1/3$ however for solution II this value of the parameter does not allow for a real solution. Both in solution I and II the parameter value $x = p = 1/2$ is a well defined solution with null magnetic field, $C_B = 0$. In solution II and IV the parameter value $x = p = 2/3$ is also a well defined solution. In solution III the particular case $p = -1$ corresponding to $x = 1/14$ ($\lambda = b^2/8$) does not allow for solutions of the equations of motion, hence this value of the parameter is excluded. In solutions III and IV the value of the parameter $x = 1/6$ corresponds to $-\infty$ and $+\infty$, respectively. In addition, for solution IV, the particular case $x = 1/2$ corresponding to $p = 1$ has the solutions for h, f, $\tilde B_*$ and ϕ given in (2.5) and (2.6), however it has the particular solution for A

$$p = 1 \;\Rightarrow\; \tilde A = C_A\,\log(r) + \theta\,,\;\; C_A = \frac{C_h\,\mathrm{sign}\,(m)}{C_f}. \tag{2.9}$$

All the solutions presented correspond to positive cosmological constant and the solutions I, II with $x \in]0, 1/6[$ and III allow for the limiting solution corresponding to empty flat Minkowski space-time, $x \to 0$, while solution II with $x \in [1/2, 2/3]$ and solution IV do not allow to obtain this limiting solution. For these solutions, the line element (2.2), re-written for the standard ADM parameterization (1.1), is $d\tilde s^2 = -f^2dt^2 + dr^2 + h^2(d\varphi + Adt)^2$ with

$$\begin{aligned}
f^2 &= \frac{C_f^2\,r^{2p-1}}{1 - r^{2p-2}\left(\tilde C_A\,r^{p-1} + \tilde\theta\right)^2}\\
h^2 &= C_h^2\,r\left(1 - r^{2p-2}\left(\tilde C_A\,r^{p-1} + \tilde\theta\right)^2\right)\\
A &= -\frac{C_f\,r^{2p-2}\left(\tilde C_A\,r^{p-1} + \tilde\theta\right)}{C_h\left(1 - r^{2p-2}\left(\tilde C_A\,r^{p-1} + \tilde\theta\right)^2\right)}
\end{aligned} \tag{2.10}$$

This metric has determinant $\sqrt{-g} = |C_f\,C_h|\,r^p$ and this parameterization is obtained directly from the map (2.4) corresponding to the duality (1.3). The non-null metric components can be computed directly from this parameterization as expressed in equation (2.3)

$$\begin{aligned}
\tilde g_{00} &= -C_f^2\,r^{2p-1}\,,\\
\tilde g_{11} &= 1\,,\\
\tilde g_{22} &= C_h^2\,r\left(1 - r^{2p-2}\,(\tilde C_A\,r^{p-1} + \tilde\theta)^2\right)\,,\\
\tilde g_{02} &= -C_f\,C_h\,r^{2p-1}\,(\tilde C_A\,r^{p-1} + \tilde\theta)\,.
\end{aligned} \tag{2.11}$$

In the above expressions we have replace the constants C_A (2.6) and θ by the respective expressions multiplied by the ratio C_f/C_h

$$\tilde{\theta} = \frac{C_f}{C_h}\,\theta \ , \ \tilde{C}_A = \frac{C_f}{C_h}\,C_A = \frac{\text{sign}\,(m)}{(1-p)}\sqrt{\frac{1-3p}{1-6x}} \ . \quad (2.12)$$

We note that for $p < 1$ the metric has ADM signature $\text{diag}(-,+,+)$ corresponding to the chosen convention while for $p > 1$ the metric has ADM signature $\text{diag}(+,+,-)$ such that further considering a radial coordinate transformation $r \to 1/r$ it is obtained the metric ADM signature $\text{diag}(+,-,-)$, hence corresponding to the opposite convention with respect to the originally chosen convention. At $p = 1$ the metric ADM signature depends on the sign of the factor $(1 - (\tilde{C}_A + \tilde{\theta})^2)$, when this factor is positive it has ADM signature $\text{diag}(-,+,+)$ and when this factor is negative (considering the coordinate transformation $r \to 1/r$) it has ADM signature $\text{diag}(+,-,-)$. We recall that the coordinate transformation $r \to 1/r$ implies exchanging the origin with spatial infinity $r : 0 \leftrightarrow +\infty$. In addition, when horizons are present this swapping of signature is equivalent to swapping the exterior region with the interior region of the horizons.

For the solutions discussed here, the swapping of the metric ADM signature with respect to the chosen convention corresponds to solution IV with the parameter x in the range $x \in]1/6, 1/2]$. Generally, for a given particular solution changing the metric ADM signature, the duality corresponding to a double Wick rotation of the coordinates t and φ (1.5) could generate new solutions which would maintain the metric ADM signature. However for the solutions just computed, when considering the reality conditions on the fields discussed in appendix 2.1, the duality (1.5) simply swaps the sign of $\hat{\epsilon}$ and the parameter p, hence no new solutions are obtained, instead solutions I and II are swapped with each other and solutions III and IV are swapped with each other.

2.2 Singularities and curvature analysis

In this section we analyze the space-time singularities, the existence of horizons and its location.

To analyze space-time singularities in 2+1-dimensions it is enough to analyze the contraction of the Ricci scalar $R_{\mu\nu}$ with itself [23]. For the solutions computed in the previous section this contraction is

$$\begin{aligned} R_{\mu\nu}R^{\mu\nu} \ = \ & \frac{1}{4r^{12}}\left[\left(3 - 16\,p + 34\,p^2 - 28\,p^3 + 8\,p^4\right)\,r^8\right. \\ & +3\tilde{C}_A^4\,(p-1)^4\,r^{8p} - 2\tilde{C}_A^2(p-1)^2\times \\ & \left.\times(4p-5)(4p-3)\,r^{4+4p}\right] \ . \end{aligned} \quad (2.13)$$

For the particular case $p = 1$ we obtain $R_{\mu\nu}R^{\mu\nu} = 3/(2r^4)$, hence for $p \geq 1$ the dominant divergent term near $r = 0$ is proportional to $\sim 1/r^4$, while for $p < 1$ it is proportional to $1/r^{12-8p}$ such that we conclude that there is a space-time singularity at $r = 0$ for all values of p. In addition, for $p > 3/2$ corresponding to $x < 9/26$ in solution IV, spatial infinity is also a space-time singularity as the dominant divergent term is proportional to $\sim r^{8p-12}$.

As for the curvature it is

$$R = \frac{-(1-6p+4p^2)\,r^4 + \tilde{C}_A^2\,(p-1)^2\,r^{4p}}{2r^6} \ . \quad (2.14)$$

For the particular case $p = 1$ the curvature is $R = 1/r^2$. Consistently with the singularity analysis discussed above, for $p < 3/2$ the curvature vanishes at spatial infinity, hence space-time is asymptotically flat, for $p = 3/2$ it converges to the positive constant $\tilde{C}_A^2/8$ and for $p > 3/2$ it diverges.

Depending on the values of x the curvature is either always positive or exist regions where it is negative. For solution I and II, it is always positive for $x \geq (8-3\sqrt{5})/38$, while for $x < (8-3\sqrt{5})/38$ it is negative for $r > r_{0.\text{I}}$ having a negative minimum value at $r = r_{\text{min.I}} > r_{0.\text{I}}$ and converging to 0 at spatial-infinity. Near the origin, for $r < r_{0.\text{I}}$, it is positive. Here $r_{0.\text{I}}$ and $r_{\text{min.I}}$ are

$$\begin{aligned} r_{0.\text{I}} \ &= \ \left(1 - 7x - 3\sqrt{x(2-3x)}\right)^{\frac{1}{4(p-1)}} \\ & \qquad \Rightarrow \ r_{0.\text{I}} \ \in]1, +\infty[\ , \\ r_{\text{min.I}} \ &= \ \left(\frac{3-45x+102x^2-(7-22x)\sqrt{x(2-3x)}}{9-26x}\right)^{\frac{1}{4(p-1)}} \\ & \qquad \Rightarrow \ r_{\text{min.I}} \ \in]3^{\frac{1}{4}}, +\infty[\ . \end{aligned} \quad (2.15)$$

For solution III the curvature is negative for $r > r_{0.\text{III}}$ having a negative minimum value at $r = r_{\text{min.III}} > r_{0.\text{III}}$, it converges to 0 at spatial-infinity and near the origin, for $r < r_{0.\text{III}}$, it is positive. As for solution IV, for $x \in]1/6, 9/26[$ ($x = 9/26$ corresponds to $p = 3/2$), the curvature is negative for $r < r_{0.\text{III}}$ and it is positive for $r > r_{0.\text{III}}$ diverging at spatial infinity, for $x = 9/26$ the curvature is negative for $r < 2/\sqrt{13}$ and it is positive for $r > 2/\sqrt{13}$ converging to 13/8 at spatial infinity, for $x \in]9/26, (8+3\sqrt{5})/38[$ it is negative near the origin for $r < r_{0.\text{III}}$ and it is positive for $r > r_{0.\text{III}}$ converging to 0 at spatial infinity and it has a positive maximum value at $r = r_{\text{min.III}} > r_{0.\text{III}}$, while for $x \in [(8+3\sqrt{5})/38, 2/3[$ the curvature is always positive converging to 0 at spatial infinity. Here $r_{0.\mathrm{III}}$ and $r_{\min.\mathrm{III}}$ are

$$\begin{aligned} r_{0.\mathrm{III}} &= \left(1-7x+3\sqrt{x(2-3x)}\right)^{\frac{1}{4(p-1)}} \\ &\Rightarrow \begin{cases} r_{0.\mathrm{III}} \in]0.93,1[\text{ for } x\in]0,\frac{1}{6}[\\ r_{0.\mathrm{III}} \in]0,1.01[\text{ for } x\in]\frac{1}{6},\frac{2}{3}[\end{cases} \\ r_{\min.\mathrm{III}} &= \left(\frac{3-45x+102x^2+(7-22x)\sqrt{x(2-3x)}}{9-26x}\right)^{\frac{1}{4(p-1)}} \\ &\Rightarrow \begin{cases} r_{\min.\mathrm{III}} \in]1,3^{\frac{1}{4}}[\text{ for } x\in]0,\frac{1}{6}[\\ r_{\min.\mathrm{III}} \in]0,1[\text{ for } x\in]\frac{9}{26},\frac{8+3\sqrt{5}}{38}[\end{cases} \end{aligned} \quad (2.16)$$

Hence, resuming the previous analysis, the curvature values for the several allowed solutions are, for the several solutions discussed,

$$\begin{aligned} &\text{I.} \quad \hat{\epsilon}=+1, \\ &\quad x\in \left]0,\tfrac{8-3\sqrt{5}}{38}\right[, \\ &\quad \Rightarrow\ R\in]R(r_{\min.\mathrm{I}})<0,+\infty[\\ &\quad x\in \left[\tfrac{8-3\sqrt{5}}{38},\tfrac{1}{2}\right] , \\ &\quad \Rightarrow\ R\in]0,+\infty[\\ &\text{II.} \quad \hat{\epsilon}=-1 , \\ &\quad x\in \left]0,\tfrac{8-3\sqrt{5}}{38}\right[, \\ &\quad \Rightarrow\ R\in]R(r_{\min.\mathrm{I}})<0,+\infty[\\ &\quad x\in \left[\tfrac{8-3\sqrt{5}}{38},\tfrac{1}{6}\right[\cup \left[\tfrac{1}{2},\tfrac{2}{3}\right] , \\ &\quad \Rightarrow\ R\in]0,+\infty[\\ &\text{III.} \quad \hat{\epsilon}=+1 , \\ &\quad x\in]0,\tfrac{1}{6}[/ \{\tfrac{1}{14}\} , \\ &\quad \Rightarrow\ R\in]R(r_{\min.\mathrm{III}})<0,+\infty[\\ &\text{IV.} \quad \hat{\epsilon}=-1 , \\ &\quad x\in]\tfrac{1}{6},\tfrac{9}{26}[, \\ &\quad \Rightarrow\ R\in]-\infty,+\infty[\\ &\quad x=\tfrac{9}{26} , \\ &\quad \Rightarrow\ R\in]-\infty,\tfrac{13}{8}[\\ &\quad x\in \left]\tfrac{9}{26},\tfrac{8+3\sqrt{5}}{38}\right[, \\ &\quad \Rightarrow\ R\in]-\infty,R(r_{\min.\mathrm{III}})>0[\\ &\quad x\in \left[\tfrac{8+3\sqrt{5}}{38},\tfrac{2}{3}\right] , \\ &\quad \Rightarrow\ R\in]0,+\infty[\end{aligned} \quad (2.17)$$

As for the nature of the space-time singularity we note that, independently of the value of the parameter p, the maximum value of the coordinate φ diverges at the singularity $r=0$ and it is finite up to spatial infinity being real outside the horizon (2.28) discussed in the next section. At spatial infinity it diverges for $p\leq -1/4$ and $p>3/2$ and it is asymptotically null for $p\in[1,3/2[$ (being finite at $p=3/2$). As for the range of the parameter $p\in]-1/4,1[$ there is a specific frame for which the maximum value of the coordinate φ matches the usual relations corresponding to flat Minkowski space-time. Specifically, defining the 2-dimensional intrinsic metric $\tilde{h}_{ij}=\mathrm{diag}(1,h^2)$ corresponding to metric $\tilde{g}_{\mu\nu}$ (2.11) and considering a rescaling of the radial coordinate

$$r=\tilde{r}^{\xi}\ \Rightarrow\ dr=\xi\,\tilde{r}^{\xi-1}\,d\tilde{r} , \quad (2.18)$$

we obtain that the maximum value for the coordinate φ is

$$\begin{aligned} \varphi_{\max} &= \frac{2\pi}{\sqrt{-|g_{\mu\nu}|}}\sqrt{\frac{h_{\varphi\varphi}}{h_{rr}}}=\frac{2\pi}{f\sqrt{h_{rr}}} \\ &= \frac{2\pi\tilde{r}^{1-\xi(2p+1/2)}}{|\xi\,C_f|}\times \\ &\quad \times\sqrt{1-\tilde{r}^{2\xi(p-1)}\left(\tilde{C}_A\tilde{r}^{\xi(p-1)}+\tilde{\theta}\right)^2} . \end{aligned} \quad (2.19)$$

such that the following asymptotic expressions at spatial infinity are obtained

$$\begin{aligned} \sqrt{-|\tilde{g}_{\mu\nu}|} &= |\xi\,C_f C_h|\,\tilde{r}^{-1+\xi(1+2p)} , \\ \lim_{r\to\infty}\sqrt{|h_{ij}|} &= |\xi\,C_h|\,\tilde{r}^{-1+\frac{3}{2}\xi} , \\ \lim_{r\to\infty}\varphi_{\max} &= \frac{2\pi}{|\xi\,C_f|}\,\tilde{r}^{1-\frac{\xi(1+4p)}{2}} . \end{aligned} \quad (2.20)$$

Setting $\xi=2/(1+4p)$, $\varphi_{\max}$ is asymptotically constant exactly matching 2π for $C_f=(1+4p)/2$. In addition we note that at spatial infinity both the space-time measure $\sqrt{-|g_{\mu\nu}|}$ and the space measure $\sqrt{|h_{ij}|}$ are, in this frame proportional to a positive exponent of $\tilde{r}$. Let us further note that the constant C_f is interpreted as the velocity of light in vacuum and its value can be redefined by a rescaling of the time coordinate t, hence there is some loss of generality when fixing the constant $C_f=(1+4p)/2$ (to ensure that $\lim_{\tilde{r}\to+\infty}\varphi=2\pi$) as we are fixing the speed of light in a particular frame, hence we are generally leaving C_f as a free constant. Resuming this discussion we conclude that the coordinate φ can exactly match the angular coordinate for Minkowski empty flat space-time at spatial infinity for a particular frame only when

$$p\in\left]-\frac{1}{4},\frac{1}{2}\right[/\{0\} , \quad (2.21)$$

When considering this constraint the range of the parameter x for solution I is not affected, for solution II is reduced to $x \in]0, 1/6[$, for solution III is reduced to $x \in]0, 1/62[$ and solution IV is excluded. We further note that for this range only the space-time singularity at the origin exists (2.22) as $p < 3/2$ such that no singularity at spatial infinity is present.

For all values of p, $\varphi_{\max}$ diverges at the singularity $r = 0$ and, for $p > 3/2$, $\varphi_{\max}$ is null at the singularity $r \to +\infty$, hence we interpreted these singularities as a decompactification singularity and a conical singularity, respectively [23]

$$\begin{array}{l} \forall_p \ , \ \lim_{r\to 0} \varphi_{\max} = +\infty \ \Rightarrow \\ \quad r = 0 \text{ is a decompactification singularity} \ . \\ \\ p > \dfrac{3}{2} \ , \ \lim_{r\to +\infty} \varphi_{\max} = 0 \ \Rightarrow \\ \quad r \to +\infty \text{ is a conical singularity} \ . \end{array} \tag{2.22}$$

Next we analyze the horizons for an external observer.

2.3 Horizons and photon topological mass

To analyze the existence of horizons the usual approach is to compute the geodesic motion of photons. From the point of view of an external observer the horizon corresponds to the spatial hyper-surface for which the photon freezes such that its geodesic equation is $\dot{r} = 0$. In [23] were computed the differential equations describing geodesic motion. For a particle with null angular momentum $L = 0$ we obtain

$$\begin{array}{rcl} \dot{r}_\kappa & = & \pm\frac{\sqrt{-g\left(-g\frac{\kappa}{E^2}+g_{22}\right)}}{g_{22}} \\ & = & \pm\frac{|C_f| r^{p-\frac{1}{2}}\sqrt{1+\frac{\kappa}{E^2}C_f^2\, r^{2p-1} - r^{2p-2}\,(\tilde{C}_A\, r^{p-1}+\tilde{\theta})^2}}{1-r^{2p-2}\,(\tilde{C}_A\, r^{p-1}+\tilde{\theta})^2} \ , \\ \dot{\varphi}_\kappa & = & -\frac{g_{02}}{g_{22}} = -\frac{C_f}{C_h} \times \frac{r^{2p-2}(\tilde{C}_A\, r^{p-1}+\tilde{\theta})}{1-r^{2p-2}(\tilde{C}_A\, r^{p-1}+\tilde{\theta})^2} \ , \end{array} \tag{2.23}$$

where $g = |g_{\mu\nu}|$ is the determinant of the metric, E the energy of the particle and $\kappa = -1$ for standard massive particles (corresponding to time-like trajectories), $\kappa = 0$ for photons or any other massless particles (corresponding to light-like trajectories) and $\kappa = +1$ for tachyons or other particles with imaginary energy eigenvalues (corresponding to space-like trajectories).

Generally the above equations are not solvable analytically. In the following we will analyze the zeros and divergences of the first equation for particles traveling towards the singularities which is enough to conclude whether a horizon exist or not. We further note that due to the Chern-Simons term the photon acquires a topological mass m such that its energy squared is $E^2 = m^2$ [35]. Specifically from the equation of motion for A_μ we obtain [23] $\partial_\alpha(\sqrt{-g}\, e^{c\phi} F^{\alpha\mu}) + m\epsilon^{\mu\alpha\beta} F_{\alpha\beta}/2 = 0$ such that computing the divergence of this equation, replacing itself in the resulting differential equation and using the definition of the dual field strength $*F^\mu = -\sqrt{-g}\, e^{c\phi}\epsilon^{\mu\alpha\beta}F_{\alpha\beta}/(2\sqrt{-g}\, e^{c\phi})$ we obtain the photon propagation equation in dual form [35]

$$\begin{array}{l} \left(\Box - m^2\right) * F^\mu = 0 \ , \\ \Box(\cdot) = \dfrac{1}{\sqrt{-g}\, e^{c\phi}}\partial_\alpha\left(\sqrt{-g}\, e^{c\phi}\partial^\alpha(\cdot)\right) \ , \end{array} \tag{2.24}$$

where $\Box$ stands for the $2+1$-dimensional Laplace operator for action (2.1) and the relative signs in this equation do depend on the metric signature convention. In particular we note that in flat space-time, for the convention adopted here, $\eta_{\mu\nu} \sim \mathrm{diag}(-,+,+)$ we consistently obtain $(-\partial_0\partial^0 + \partial_i\partial^i - m^2) * F^\mu = 0$ while for the opposite sign convention [35] $\eta_{\mu\nu} \sim \mathrm{diag}(+,-,-)$ we obtain $(\Box + m^2) * F^\mu = (\partial_0\partial^0 - \partial_i\partial^i + m^2) * F^\mu = 0$ such that both equations are the same up to an overall minus sign, corresponding to a photon with a standard (topological) mass m. Hence as extensively analyzed in the literature we conclude that no massless photons exist for Maxwell Chern-Simons theories [34, 35].

It is straight forward to check that for all values of p and κ, as we approach the singularity at $r = 0$, the velocity of any given particle vanishes

$$\lim_{r\to 0} \dot{r}_\kappa = 0 \ , \tag{2.25}$$

while in this limit $\dot{\varphi}_\kappa$ is finite for $p = 1$ and null for all other values of p. This implies that the singularity is itself an horizon, hence it is not a naked singularity. However this result is not conclusive as for higher values of $r > 0$ there exists a divergence of $\dot{r}_\kappa$, specifically when the denominator of the first equation of (2.23) is null the particle velocity diverges. This divergence is located at the value of the radial coordinate $r = r_{\mathrm{div}}$ obeying the equation

$$1 = \left(r_{\mathrm{div}}^{p-1}\,(\tilde{C}_A\, r_{\mathrm{div}}^{p-1} + \tilde{\theta})\right)^2 \ . \tag{2.26}$$

This equation has one real positive solution r_{div} for all values of p and $\tilde{\theta}$. We recall that $\tilde{C}_A$ is not a free constant being expressed in equation (2.6) and (2.12) as a function of x and $p = p(x)$. Specifically, one of the 4 solution $r_{\mathrm{div},\pm,\pm} = ((-\tilde{\theta} \pm \sqrt{\tilde{\theta}^2 \pm 4\tilde{C}_A})/(2\tilde{C}_A))^{\frac{1}{p-1}}$, is real and positive for all the allowed range of the parameters.

In addition to ensure that for $r > r_{\mathrm{div}}$, the space-time has Minkowski signature $\mathrm{diag}(-,+,+)$ and that $\dot{r}_\kappa$ describes the geodesic motion of a particle it is required that this quantity ($\dot{r}_\kappa$) be real valued and consistently have either positive sign for particles traveling away from the singularity either negative sign for particles traveling towards the singularity. These properties are obeyed as long as the factor $1 - \left(r^{p-1}\,(\tilde{C}_A\, r^{p-1} + \tilde{\theta})\right)^2$ is real and positive for $r > r_{\mathrm{div}}$. This statement is simply equivalent to the bound $p < 1$ such that the factor

$\left(r^{p-1}\left(\tilde{C}_A\, r^{p-1}+\tilde{\theta}\right)\right)^2$ decreases with growing radial coordinate. Hence we obtain the bounds

$$\left\{\begin{array}{lll} r & > & r_{\rm div} \\ 1 & > & \left(r^{p-1}\left(\tilde{C}_A\, r^{p-1}+\tilde{\theta}\right)\right)^2 \end{array}\right. \Leftrightarrow p<1\ . \qquad (2.27)$$

This bound, $p<1$, is consistent with the analysis in the previous section.

For massless particles the velocity divergence in $\dot{r}_{\kappa=0}$ just analyzed is outside any horizon. This is straight forwardly shown by noting that for $\kappa=0$ the numerator of $\dot{r}_{\kappa=0}$ is the square root of its denominator (2.23) such that the only horizon is at $r=0$ as already concluded (2.25). Classically there is no interpretation for a particle velocity divergence, however we note that upon path integral quantization this phenomena can be consistently described as a tunneling effect, hence an instanton configuration [26]. We are not proceeding with this analysis here, instead let us note that from the photon equations of motion (2.24) the photon acquires a topological mass m such that no massless photons exist in the theory discussed here. Therefore, assuming that no massless particles exist in the theory let us analyze the photon geodesic motion with energy squared given by $E^2=m^2$ and light-like trajectories ($\kappa=-1$). For this case we conclude that an horizon at the value of the radial coordinate for which the numerator of $\dot{r}_{\kappa=-1}$ is null. Furthermore we note that, due to the denominator of $\dot{r}_{\kappa=-1}$ being positive for $r>r_{\rm div}$ and the term $\kappa C_f^2/E^2 r^{2p-1}=-C_f^2\, r^{2p-1}/m^2<0$ being negative for all values of r, the value of the radial coordinate corresponding to the horizon $r=r_{\rm H}$ is greater than $r_{\rm div}$ (2.26)

$$\left\{\begin{array}{lll} p & < & 1 \\ 1 & = & \left(r_{\rm H}^{p-1}\left(\tilde{C}_A\, r_{\rm H}^{p-1}+\tilde{\theta}\right)\right)^2+\dfrac{C_f^2}{m^2}\, r_{\rm H}^{2p-1} \end{array}\right. \Leftrightarrow\ r_{\rm H}>r_{\rm div}\ . \qquad (2.28)$$

Although the author failed to find a analytical solution for this equation the previous discussion is enough to conclude that for all allowed solutions and parameter ranges with $p<1$ there exists an horizon for the value of the radial coordinate $r_{\rm H}$ given by this equation. Hence both the space-time singularity at $r=0$ and the singularity in the particle velocity at $r=r_{\rm div}$ are inside the horizon and are not observable by an external observer. This is a valid statement both for photons (which are massive due to the Chern-Simons term) and for any other massive particles.

As for the particular case of solution IV with $p>1$ we note that (further considering the redefinition $r\to 1/r$) the ADM signature of the metric for $r>r_H$ (2.28) is ${\rm diag}(+,-,-)$, hence with the opposite sign of the original convention. Recalling that at the horizon the metric changes sign [51], this is simply interpreted as that the interior of the horizon for $p>1$ corresponds to the region with $r>r_H$, hence for an external observer in the region $r\in]0,r_H[$ these solutions are interpreted as a dressed point-like singularity at $r=0$ and an horizon at $r=r_H$ such that $r_{\rm div}>r_H$ and the singularity at $r=+\infty$ are within the region contained by the horizon ($r>r_H$).

Next we compute the mass, the magnetic flux and the angular momentum for the classical solutions obtained.

2.4 Mass, Angular Momentum and Magnetic Flux

In this section we derive and analyze the expressions for the mass, angular momentum and magnetic flux for the solutions computed (2.8). We postpone a interpretation of these results until the next section 3 where all the possible cases are gathered in table 1 and the results obtained are discussed.

We recall that there are several definitions of mass, namely in [23] it was computed the ADM mass [51, 52, 59]. Adopting this definition of mass, for the metric parameterization (1.1), it is obtained

$$M_{\rm ADM}=2h'+4\lambda h\phi\phi'+2\hat{\epsilon}he^{-b\phi/2}A_\varphi A'_\varphi\Big|_{r\to\delta_M}^{r\to\infty}\ , \qquad (2.29)$$

where δ_M is a cut-off near the singularity (of order of the Planck Length) introduced to regularize the singularity at the origin maintaining the mass value finite. However for the magnetic solutions (2.5) the value of the ADM mass is generally complex. We note that the ADM mass corresponds to the (classical) eigenvalue of the Hamiltonian constraint, hence, generally, aiming at the quantization of the gravitational sector of the theory. This is not the aiming of the present discussion. Instead of the ADM definition of mass we are taking a classical definition of mass that allows for real values to the solutions (2.5). The standard General Relativity definition of mass is the integral of the gravitational mass-energy density ρ_g. For a generic Einstein Tensor $G_{\mu\nu}$ the mass-energy density ρ_g and pressure p_g are [51]

$$\rho_g=G_{00}-p_g(1-g_{00})\quad,\quad p_g=-\frac{G_{03}}{g_{03}}\ , \qquad (2.30)$$

such that the total mass and angular momentum are obtained by integrating these quantities over a spatial hyper-surface [51]

$$\begin{array}{lll} M & = & \displaystyle\int\sqrt{|h_{ij}|}\,\rho_g\, dx^2\ , \\ S_z & = & \displaystyle\int\sqrt{|h_{ij}|}\, r\, p_g\, g^{03}\, dx^2\ , \end{array} \qquad (2.31)$$

where $|h_{ij}|$ stands for the determinant of the induced 2-dimensional spatial metric discussed in the previous section and we note that in $2+1$-dimensions the only angular momentum component correspond to the $3+1$-dimensional angular momentum along z (from the definition $S_k=\int\epsilon_{kij}x^iT^{0j}$ [51] it is obtained that $S_r=S_\varphi=0$).

For the action (2.1) there is also a contribution to the classical gravitational mass due to the dilaton-like scalar field ϕ. This contribution can be read directly from the Einstein Equations [23]

$$G_{\mu\nu} + \lambda \partial_\mu \phi \partial_\nu \phi - \frac{\lambda}{2} g_{\mu\nu} \partial_\alpha \phi \partial^\alpha \phi + \frac{1}{2} e^{b\phi} g_{\mu\nu} \Lambda = 2 e^{-\frac{b}{2}\phi} T_{\mu\nu} \; , \tag{2.32}$$

where we have taken in consideration the ansatz $a = 0$, $c = -b/2$ and the bare electro-magnetic stress-energy tensor is $T_{\mu\nu} = \hat{\epsilon} \left(F_{\mu\alpha} F_\mu{}^\alpha - g_{\mu\nu} F^2/4 \right)$. Hence we note that, for a classical configuration obeying these equations, the Einstein tensor contribution plus the scalar field contribution to the gravitational mass-energy density and pressure matches the respective electromagnetic quantities [51]

$$\begin{aligned} \rho_{grav} &= \rho_g + \rho_\phi = \rho_{EM} \; , \\ p_{grav} &= p_g + p_\phi = p_{EM} \; . \end{aligned} \tag{2.33}$$

In the following we employ these definitions of gravitational energy-momentum density and pressure density to compute the respective total quantities. Noting that the only non-null component of the Maxwell tensor is $F_{r\varphi} = F_{12} = \tilde{B}_*$ (2.5) it is straight forward to obtain the expressions for these quantities

$$\begin{aligned} \rho_{grav} = \rho_{EM} &= -\frac{\hat{\epsilon}}{2} g_{00} g^{11} g^{22} \tilde{B}_*^2 \, e^{-\frac{b}{2}\phi} - p_{EM}(1 - g_{00}) \\ &= -\frac{\hat{\epsilon}\, C_B^2 \, C_\phi}{2 C_h^2} r^{2p-4} \; , \\ p_{grav} = p_{EM} &= \frac{\hat{\epsilon}}{2} g^{11} g^{22} \tilde{B}_*^2 \, e^{-\frac{b}{2}\phi} \\ &= \frac{\hat{\epsilon} C_B^2 \, C_\phi}{2 C_h^2} r^{2p-4} \; . \end{aligned} \tag{2.34}$$

These quantities are real valued for all the range of the parameter p and in the limit $p \to 0$ are consistently null, as already discussed the particular solution corresponding to $p = 0$ corresponds to Minkowski flat empty spacetime. We also note that the equation of state for these solutions is a constant $\omega_{grav} = \rho_{grav}/p_{grav} = -1$. However, depending on the value of the parameter p they may have either a divergence at the origin $r \to 0$ (IR), either a divergence at spatial infinity $r \to +\infty$ (UV) or both.

To regularize these divergences and allow for a simpler analysis of the total quantities we consider two cutoffs δ_{IR} (lower cut-off) and δ_{UV} (upper cut-off) which can be taken to 0 and $+\infty$, respectively. Specifically for the mass M we obtain the following integral expression

$$\begin{aligned} M &= \int_{\delta_{IR}}^{\delta_{UV}} dr \int_0^{\varphi_{\max}} d\varphi \sqrt{|h_{ij}|}\, \rho_{grav} \\ &= -\frac{\hat{\epsilon} C_B^2 C_\phi \pi}{|C_f C_h|} \int_{\delta_{IR}}^{\delta_{UV}} dr \, r^{p-3} \times \\ &\quad \left(1 - r^{2p-2} (\tilde{C}_A \, r^{p-1} + \tilde{\theta})^2 \right) \; , \end{aligned} \tag{2.35}$$

and for the angular momentum S_z

$$\begin{aligned} S_z &= \int_{\delta_{IR}}^{\delta_{UV}} dr \int_0^{\varphi_{\max}} d\varphi \sqrt{|h_{ij}|}\, r \, p_{grav} \, g^{02} \\ &= -\frac{\hat{\epsilon} C_B^2 C_\phi \pi}{(C_f C_h)^2} \int_{\delta_{IR}}^{\delta_{UV}} dr \, r^{p-3} \left(\tilde{C}_A \, r^{p-1} + \tilde{\theta} \right) \times \\ &\quad \times \left(1 - r^{2p-2} (\tilde{C}_A \, r^{p-1} + \tilde{\theta})^2 \right) \; . \end{aligned} \tag{2.36}$$

We note that these quantities are evaluated in a 2-dimensional spatial hyper-plane, hence M has units of mass over length and S_z of mass such that when embedded into a 3-dimensional spatial manifold it is further required to integrated over the thickness of the 2-dimensional embedding along the orthogonal direction (z) to retrieve the standard 3-dimensional quantities with units of mass and angular momentum, respectively. It is relevant to stress that, as discussed in [50], from a $3+1$-dimensional perspective these computations are valid and consistent only for systems with constant fields along the direction orthogonal to the planar system as it is the case of systems with cylindrical symmetry (for further discussions on embedded $2+1$-dimensional systems see for example [14] and [63]).

Evaluating the integral expression (2.35) for the Mass M we obtain

$$\begin{aligned} p &\neq -1, 1, \frac{6}{5}, \frac{4}{3}, \frac{5}{4}, 2 \\ M &= -\frac{\hat{\epsilon} C_B^2 C_\phi \pi}{|C_f C_h|} \left(\frac{\tilde{C}_A^2}{6 - 5p} r^{5p-6} + \frac{2 \tilde{C}_A \tilde{\theta}}{5 - 4p} r^{4p-5} \right. \\ &\quad \left. + \frac{\tilde{\theta}^2}{4 - 3p} r^{3p-4} + \frac{1}{p-2} r^{p-2} \right)_{\delta_{IR}}^{\delta_{UV}} \; . \end{aligned} \tag{2.37}$$

For $p = -1$ there are no allowed solution and the specific expressions for $p = 1, 6/5, 4/3, 5/4, 2$ are listed in appendix B in equations (B.1–B.5). By direct inspection of the expressions for the mass it is straight forward to conclude that the divergence at the origin $r \to 0$ is present for $p \leq 2$ and that the divergence at spatial infinity $r \to +\infty$ is present for $p \geq 6/5$. Hence, depending on the value of the parameter p, finite mass expressions M can be evaluated by considering the following limits on δ_{IR} and δ_{UV}

$$\begin{aligned} p &\in \left] -\infty, \frac{6}{5} \right[/ \{-1, 0\} & \Rightarrow & \left\{ \begin{array}{ccc} \delta_{IR} & \not\to & 0 \\ \delta_{UV} & \to & +\infty \end{array} \right. \\ p &\in \left[\frac{6}{5}, 2 \right] & \Rightarrow & \left\{ \begin{array}{ccc} \delta_{IR} & \not\to & 0 \\ \delta_{UV} & \not\to & +\infty \end{array} \right. \\ p &\in \left] 2, +\infty \right] & \Rightarrow & \left\{ \begin{array}{ccc} \delta_{IR} & \to & 0 \\ \delta_{UV} & \not\to & +\infty \end{array} \right. \end{aligned} \tag{2.38}$$

The first range for the parameter p corresponds to solutions I, II, III and IV with $p \in]2/3, 6/5[$ (2.8) while the second and third ranges correspond to solution IV.

As for the sign of the mass, for the range $p \in]-\infty, 1]/\{-1, 0\}$ it has the opposite sign of $\hat{\epsilon}$, $M \sim -\hat{\epsilon}$ and for the range $p \in]1, +\infty[$ it has the same sign of $\hat{\epsilon}$, $M \sim \hat{\epsilon}$. We note that a negative mass is not unexpected since we are allowing for a gauge ghost sector, we recall that $\hat{\epsilon} = +1$ corresponds to a ghost gauge sector and that $\hat{\epsilon} = -1$ corresponds to a standard gauge sector. For the range $p \in]-\infty, 1[$, outside the horizon ρ_{grav} has the opposite sign of $\hat{\epsilon}$ in accordance to whether the gauge sector is a ghost or a standard sector, however the predominant contribution to the value of the mass is within the horizon and the integrand in (2.35) changes sign at the horizon such that the total mass is actually positive when it is considered a ghost gauge sector and it is negative when a standard ghost gauge sector is considered. in the range $p \in]1, +\infty[$ the opposite behavior is verified such that the total mass is negative when it is considered a ghost gauge sector and it is positive when a standard ghost gauge sector is considered. This is simply explained as due to the contribution of the scalar field to the total mass, its classical energy opposes the contribution from the standard gravitational sector.

Evaluating the integral expression (2.36) for the angular momentum S_z we obtain

$$
\begin{aligned}
p &\neq -1,\, 1,\, \frac{7}{6},\, \frac{6}{5},\, \frac{5}{4},\, \frac{4}{3},\, \frac{3}{2},\, 2 \\
S_z &= -\frac{\hat{\epsilon} C_B^2 C_\phi \pi}{(C_f C_h)^2} \left(\frac{\tilde{C}_A^3}{7-6p}\, r^{6p-7} + \frac{3\tilde{C}_A^2 \tilde{\theta}}{6-5p}\, r^{5p-6} \right. \\
&\quad + \frac{3\tilde{C}_A \tilde{\theta}^2}{5-4p}\, r^{4p-5} + \frac{\tilde{\theta}^3}{4-3p}\, r^{3p-4} \\
&\quad \left. + \frac{\tilde{C}_A}{3-2p}\, r^{2p-3} + \frac{\tilde{\theta}}{p-2}\, r^{p-2} \right)_{\delta_{IR}}^{\delta_{UV}} .
\end{aligned}
\tag{2.39}
$$

The specific expressions for $p = -1,\ 7/6,\ 6/5,\ 5/4,\ 4/3,\ 3/2,\ 2$ are listed in appendix B in equations (B.6–B.12). By direct inspection of the expressions for the angular momentum it is straight forward to conclude that the divergence at the origin is present for $p \leq 2$ and that the divergence at spatial infinity is present for $p \geq 7/6$. Hence, depending on the value of the parameter p, finite angular momentum expressions S_z can be evaluated by considering the following limits on δ_{IR} and δ_{UV}

$$
\begin{aligned}
p &\in \left]-\infty, \frac{7}{6}\right[/ \{-1, 0\} && \Rightarrow \begin{cases} \delta_{IR} \not\to 0 \\ \delta_{UV} \to +\infty \end{cases} \\
p &\in \left[\frac{7}{6}, 2\right] && \Rightarrow \begin{cases} \delta_{IR} \not\to 0 \\ \delta_{UV} \not\to +\infty \end{cases} \\
p &\in\ ]2, +\infty] && \Rightarrow \begin{cases} \delta_{IR} \to 0 \\ \delta_{UV} \not\to +\infty \end{cases}
\end{aligned}
\tag{2.40}
$$

Similarly to the results obtained for the mass, the first range for the parameter p corresponds to solutions I, II, III and IV with $p \in]2/3, 7/6[$ (2.8) while the second and third ranges correspond to solution IV.

As for the sign of the angular momentum S_z we obtain that in the range $p \in]-\infty, 1[/\{-1, 0\}$ it is $S_z \sim +\hat{\epsilon}\,\mathrm{sign}\,(\tilde{C}_A)$ which correspond to solution III in the range $p \in]-\infty, 0[/\{-1\}$, solution I and II in the range $p \in]0, 2/3[$ and solution IV in the range $p \in]2/3, 1[$. For all these cases $\tilde{C}_A \sim \mathrm{sign}\,(m)$ such that the sign of the angular momentum is $S_z \sim +\hat{\epsilon}\,\mathrm{sign}\,(m)$. For $p = 1$ we obtain that $S_z \sim -\hat{\epsilon}\,\mathrm{sign}\,(m)$. In the range $p \in]1, 1.2857[$ with $\tilde{\theta} \neq 0$ it is $S_z \sim -\hat{\epsilon}\,\mathrm{sign}\,(\tilde{\theta})$ corresponding to the solution IV. When $\tilde{\theta} = 0$, in the range $p \in]1, 5/4[$ it is $S_z \sim -\hat{\epsilon}\,\mathrm{sign}\,(\tilde{C}_A)$ for which $\tilde{C}_A \sim -\mathrm{sign}\,(m)$ such that $S_z \sim +\hat{\epsilon}\,\mathrm{sign}\,(m)$, for $p = 5/4$ it is $S_z \sim -\hat{\epsilon}\,\mathrm{sign}\,(\tilde{C}_A(1-\tilde{C}_A^2))$ for which $\tilde{C}_A = -\sqrt{31}\,\mathrm{sign}\,(m)$ such that $\tilde{C}_A(1-\tilde{C}_A^2) = 30\sqrt{31}\,\mathrm{sign}\,(m)$, hence $S_z \sim -\hat{\epsilon}\,\mathrm{sign}\,(m)$ and in the range $p \in]5/4, 1.2857[$ it is $S_z \sim +\hat{\epsilon}\,\mathrm{sign}\,(\tilde{C}_A)$ for which $\tilde{C}_A = -\mathrm{sign}\,(m)$ such that $S_z \sim -\hat{\epsilon}\,\mathrm{sign}\,(m)$. In the range $p \in [1.2857, +\infty[$ it is $S_z \sim +\hat{\epsilon}\,\mathrm{sign}\,(\tilde{C}_A)$ corresponding to solution IV with $\tilde{C}_A \sim -\mathrm{sign}\,(m)$, hence we obtain $S_z \sim -\hat{\epsilon}\,\mathrm{sign}\,(m)$.

As for the magnetic flux we note that for action (2.1) the equations of motion are expressed in terms of the covariant electro-magnetic fields $\mathcal{B} = \sqrt{-g}e^{c\phi}\tilde{B}_*$ and $\mathcal{E} = \sqrt{-g}e^{c\phi}\tilde{E}_*$ instead of the bare electro-magnetic fields $\tilde{B}_*$ and $\tilde{E}_*$ [51] and that for stationary solutions (not depending explicitly on the time coordinate) the Bianchi identities for the Maxwell tensor can also be reexpressed with respect to these quantities. Hence the Maxwell equations are defined by the covariant fields $\mathcal{B}$ and $\mathcal{E}$ such that the measurable magnetic field is $\mathcal{B}$ and its integral over the 2-dimensional manifold is

$$
\begin{aligned}
\Phi_{\mathcal{B}} &= \int_{\delta_{IR}}^{\delta_{UV}} dr \int_0^{\varphi_{max}} d\varphi \sqrt{|h_{ij}|}\sqrt{-g}e^{c\phi}\tilde{B}_* \\
&= 2C_B C_\phi C_h^2 \pi \int_{\delta_M}^{+\infty} dr\, r^p \times \\
&\quad \left(1 - r^{2p-2}\left(\tilde{C}_A\, r^{p-1} + \tilde{\theta}\right)\right) .
\end{aligned}
\tag{2.41}
$$

Evaluating this integral expression we obtain

$$\begin{aligned} p &\neq -1,\,1,\,\frac{1}{3},\,\frac{3}{5}\,, \\ \Phi_{\mathcal{B}} &= 2C_B C_\phi C_h^2 \pi \left(\frac{1}{1+p}\,r^{p+1} + \frac{\tilde{\theta}^2}{1-3p}\,r^{3p-1} \right. \\ &\left. + \frac{\tilde{\theta}\tilde{C}_A}{1-2p}\,r^{4p-2} + \frac{\tilde{C}_A^2}{3-5p}\,r^{5p-3} \right)_{\delta_{IR}}^{\delta_{UV}} . \end{aligned} \tag{2.42}$$

The expressions for the particular values of $p = 1,\,1/3,\,3/5$ are listed in appendix B in equations (B.13–B.15). Again, depending on the value of the parameter p, finite magnetic flux expressions $\Phi_{\mathcal{B}}$ can be evaluated by considering the following limits on δ_{IR} and δ_{UV}

$$\begin{aligned} p &\in\ ]-\infty,-1[&& \Rightarrow \left\{ \begin{array}{ccc} \delta_{IR} & \not\to & 0 \\ \delta_{UV} & \to & +\infty \end{array} \right. \\ p &\in \left]-1,\frac{3}{5}\right] /\{0\} && \Rightarrow \left\{ \begin{array}{ccc} \delta_{IR} & \not\to & 0 \\ \delta_{UV} & \not\to & +\infty \end{array} \right. \\ p &\in \left]\frac{3}{5},+\infty\right[&& \Rightarrow \left\{ \begin{array}{ccc} \delta_{IR} & \to & 0 \\ \delta_{UV} & \not\to & +\infty \end{array} \right. \end{aligned} \tag{2.43}$$

The first range for the parameter p corresponds to solution III, the second range to solution I, solution II with $p \in]0,1/3[\cup[1/2,3/5]$ and solution III with $p \in]-1,0[$ while the third range corresponds to solution II with $p \in]3/5,2/3]$ and solution IV (2.8).

As for the sign of the magnetic flux $\Phi_{\mathcal{B}}$ let us note that the sign of C_ϕ and C_B are independent of the specific value of the parameter p. C_ϕ is always positive, however from the classical solutions of the equations of motion the sign of C_B is arbitrary, this is simply understood by noting that, in the absence of a electric field the Einstein equations (A.10–A.13) only depend on the square of the magnetic field and that the Maxwell equations (A.8) and (A.9) with null electric field $\tilde{E} = 0$ are invariant under a change of sign of the magnetic field $\tilde{B} \to -\tilde{B}$. Hence only solutions with both non-null electric and magnetic fields are actually sensitive to the relative electromagnetic fields direction (hence the polarization of the electromagnetic fields), both through the Maxwell equations and the '02' Einstein equation. For the specific expressions of the constants given in (2.6) the choice of the magnetic field sign can be selected by choosing the sign of the free constant C_h which has no consequences at classical level, hence we will proceed our analysis leaving the sign of C_B unspecified. In the range $p \in]-\infty,1/3[$ the magnetic flux sign is $\Phi_{\mathcal{B}} \sim -\,\mathrm{sign}\,(C_B)$, for $p = 1/3$ it is $\Phi_{\mathcal{B}} \sim \mathrm{sign}\,(C_B(1-\tilde{C}_A))$ corresponding to solution I for which $\tilde{C}_A = \sqrt{3}/2$ such that $\Phi_{\mathcal{B}} \sim +\,\mathrm{sign}\,(C_B)$, in the range $p \in]1/3,1[$ it is $\Phi_{\mathcal{B}} \sim +\,\mathrm{sign}\,(C_B)$ and in the range $p \in [1,+\infty[$ it is $\Phi_{\mathcal{B}} \sim -\,\mathrm{sign}\,(C_B)$.

Next we gather all the results obtained for the solutions (2.5) and discuss possible interpretations for these configurations.

3 Discussion of results

3.1 Summary of results

In this work, based on the space-time duality (1.3) discussed in a previous publication [50] and resumed in the introduction we have computed the classical solutions listed in equations (2.5-2.8) for the gravitational fields, a scalar field and the gauge fields of Einstein Maxwell Chern-Simons theory described by action (2.1) with a non-trivial magnetic field and null electric field. We have analyzed the space-time singularities of such classical configurations and the curvature values in section 2.1; the existence of horizons taking in consideration that no massless photons exist in this theory due to the topological mass for the photon in section 2.3, concluding that a geodesic divergence is present in the interior of the horizon, hence not observable by an external observer; and in section 2.4 were derived the mass, angular momentum and magnetic flux for such configurations. We summarize all these results in table 1 as a function of the parameter $p \in]-\infty,+\infty[/\{-1\}$.

In the first column of table 1 are listed the several ranges for the value of the parameter p, in the column labeled $\lim_{r\to+\infty}\varphi_{\max}$ are listed the asymptotic finite values at spatial infinity of the maximum value for the coordinate φ which simultaneously allow the space-time measure and space measure to have as the asymptotic leading term (also at spatial infinity) a positive exponent of the radial coordinate, in the columns labeled M_{div}, $S_{z,\mathrm{div}}$ and $\Phi_{B,\mathrm{div}}$ is listed whether the mass is divergent near the origin (IR divergence) or the mass is divergent at spatial infinity (UV divergence) in accordance to the results obtained in equations (2.38), (2.40) and (2.43), respectively, in the columns labeled $\mathrm{sign}\,(M)$, $\mathrm{sign}\,(S_z)$ and $\mathrm{sign}\,(\Phi_{\mathcal{B}})$ are listed the sign for these quantities evaluated from the respective expressions (2.37), (2.39) and (2.42) as well as the particular cases listed in appendix B, in the column labeled $\lim_{r\to+\infty} R$ are listed the asymptotic values of the curvature at spatial infinity obtained by inspection of the curvature (2.14) and summarized in (2.17), in the column labeled "Singularities"are listed the location of the space-time singularities obtained by inspection of the scalar invariant $R_{\mu\nu}R^{\mu\nu}$ (2.13) and summarized in (2.22), in the column labeled "Horizons"it is listed whether the horizon at $r = 0$ and $r = r_H$ (2.28) exists according to the discussion in section 2.3, in the column labeled "Signature"are listed the ADM signatures for the metric for values of the radial coordinate above the horizon $r > r_H$ (2.28) obtained from inspection of the mapped gravitational fields f, h and A given in (2.10) corresponding to the standard ADM metric parameterization (1.1) and finally in the last column labeled "Solution"are listed the correspondence to the solutions of type I, II, III and IV summarized in equation (2.8) for each of the ranges for the values of the parameter p.

p	$\lim_{\tilde{r}\to\infty} \varphi_{\max}$ (2.20)	M_{div} (2.38)	$S_{z,\text{div}}$ (2.40)	$\Phi_{\mathcal{B},\text{div}}$ (2.43)	$\text{sign}\,(M)$ (2.37)	$\text{sign}\,(S_z)$ (2.39)	$\text{sign}\,(\Phi_{\mathcal{B}})$ (2.42)	$\lim_{\tilde{r}\to\infty} R$ (2.14)	Singularities (2.13)	Horizon (2.28)	Signature, $r > r_H$ (2.10)	Solution (2.8)
$\in\,]-\infty, -1[$	-	IR	IR	IR	$+\hat{\epsilon}$	$+\hat{\epsilon}\,\text{sign}\,(m)$	$-\,\text{sign}\,(C_B)$	0	$r = 0$	$\exists_{r=0},\ \exists_{r>0}$	$(-,+,+)$	III(Ghost)
$\in\,\left]-1, -\frac{1}{4}\right]$	-	IR	IR	IR/UV	$+\hat{\epsilon}$	$+\hat{\epsilon}\,\text{sign}\,(m)$	$-\,\text{sign}\,(C_B)$	0	$r = 0$	$\exists_{r=0},\ \exists_{r>0}$	$(-,+,+)$	III(Ghost)
$\in\,\left]-\frac{1}{4}, 0\right[$	$\frac{1+4p}{C_f}$	IR	IR	IR/UV	$+\hat{\epsilon}$	$+\hat{\epsilon}\,\text{sign}\,(m)$	$-\,\text{sign}\,(C_B)$	0	$r = 0$	$\exists_{r=0},\ \exists_{r>0}$	$(-,+,+)$	III(Ghost)
$= 0$	-	-	-	-	-	-	-	-	-	-	empty flat Minkowski	
$\in\,\left]0, \frac{1}{3}\right[$	$\frac{1+4p}{C_f}$	IR	IR	IR/UV	$+\hat{\epsilon}$	$+\hat{\epsilon}\,\text{sign}\,(m)$	$-\,\text{sign}\,(C_B)$	0	$r = 0$	$\exists_{r=0},\ \exists_{r>0}$	$(-,+,+)$	I(Ghost) and II
$\in\,\left[\frac{1}{3}, \frac{1}{2}\right[$	$\frac{1+4p}{C_f}$	IR	IR	IR/UV	$+\hat{\epsilon}$	$+\hat{\epsilon}\,\text{sign}\,(m)$	$+\,\text{sign}\,(C_B)$	0	$r = 0$	$\exists_{r=0},\ \exists_{r>0}$	$(-,+,+)$	I(Ghost)
$= \frac{1}{2}$	-	=0	=0	=0	$= 0$	$= 0$	$= 0$	0	$r = 0$	$\exists_{r=0},\ \exists_{r>0}$	$(-,+,+)$	I(ghost) and II
$\in\,\left]\frac{1}{2}, \frac{3}{5}\right]$	-	IR	IR	IR/UV	$+\hat{\epsilon}$	$+\hat{\epsilon}\,\text{sign}\,(m)$	$+\,\text{sign}\,(C_B)$	0	$r = 0$	$\exists_{r=0},\ \exists_{r>0}$	$(-,+,+)$	II
$\in\,\left]\frac{3}{5}, \frac{2}{3}\right[$	-	IR	IR	UV	$+\hat{\epsilon}$	$+\hat{\epsilon}\,\text{sign}\,(m)$	$+\,\text{sign}\,(C_B)$	0	$r = 0$	$\exists_{r=0},\ \exists_{r>0}$	$(-,+,+)$	II
$= \frac{2}{3}$	-	IR	IR	UV	$+\hat{\epsilon}$	$+\hat{\epsilon}\,\text{sign}\,(m)$	$+\,\text{sign}\,(C_B)$	0	$r = 0$	$\exists_{r=0},\ \exists_{r>0}$	$(-,+,+)$	II and IV
$\in\,\left]\frac{2}{3}, 1\right[$	-	IR	IR	UV	$+\hat{\epsilon}$	$+\hat{\epsilon}\,\text{sign}\,(m)$	$+\,\text{sign}\,(C_B)$	0	$r = 0$	$\exists_{r=0},\ \exists_{r>0}$	$(-,+,+)$	IV
$= 1$	-	IR	IR	UV	$+\hat{\epsilon}$	$-\hat{\epsilon}\,\text{sign}\,(m)$	$-\,\text{sign}\,(C_B)$	0	$r = 0$	$\exists_{r=0},\ \nexists_{r>0}$	$(+,-,-)$	IV
$\in\,\left]1, \frac{7}{6}\right[$	-	IR	IR	UV	$-\hat{\epsilon}$	$-\hat{\epsilon}\,\text{sign}\,(\tilde{\theta})$	$-\,\text{sign}\,(C_B)$	0	$r = 0$	$\exists_{r=0},\ \nexists_{r>0}$	$(+,-,-)$	IV
$\in\,\left[\frac{7}{6}, \frac{6}{5}\right[$	-	IR	IR/UV	UV	$-\hat{\epsilon}$	$-\hat{\epsilon}\,\text{sign}\,(\tilde{\theta})$	$-\,\text{sign}\,(C_B)$	0	$r = 0$	$\exists_{r=0},\ \nexists_{r>0}$	$(+,-,-)$	IV
$\in\,\left[\frac{6}{5}, 1.2857\right[$	-	IR/UV	IR/UV	UV	$-\hat{\epsilon}$	$-\hat{\epsilon}\,\text{sign}\,(\tilde{\theta})$	$-\,\text{sign}\,(C_B)$	0	$r = 0$	$\exists_{r=0},\ \nexists_{r>0}$	$(+,-,-)$	IV
$\in\,\left[1.2857, \frac{3}{2}\right[$	-	IR/UV	IR/UV	UV	$-\hat{\epsilon}$	$-\hat{\epsilon}\,\text{sign}\,(m)$	$-\,\text{sign}\,(C_B)$	0	$r = 0$	$\exists_{r=0},\ \nexists_{r>0}$	$(+,-,-)$	IV
$= \frac{3}{2}$	-	IR/UV	IR/UV	UV	$-\hat{\epsilon}$	$-\hat{\epsilon}\,\text{sign}\,(m)$	$-\,\text{sign}\,(C_B)$	$\frac{\tilde{C}_A^2}{8}$	$r = 0$	$\exists_{r=0},\ \nexists_{r>0}$	$(+,-,-)$	IV
$\in\,\left]\frac{3}{2}, 2\right]$	-	IR/UV	IR/UV	UV	$-\hat{\epsilon}$	$-\hat{\epsilon}\,\text{sign}\,(m)$	$-\,\text{sign}\,(C_B)$	$+\infty$	$r = 0, +\infty$	$\exists_{r=0},\ \nexists_{r>0}$	$(+,-,-)$	IV
$\in\,]2, +\infty[$	-	UV	UV	UV	$-\hat{\epsilon}$	$-\hat{\epsilon}\,\text{sign}\,(m)$	$-\,\text{sign}\,(C_B)$	$+\infty$	$r = 0, +\infty$	$\exists_{r=0},\ \nexists_{r>0}$	$(+,-,-)$	IV

Tabela 1: Resume of solutions as a function of the parameter p.

3.2 Conclusions

Given the solutions summarized in table 1 we proceed to interpret them physically. Of particular relevance are the divergences of the physical properties of the classical configurations, namely the total mass M, the total angular momentum J_z and the total magnetic flux $\Phi_{\mathcal{B}}$. A divergence near the space-time singularity (or singularities) is non uncommon in $2+1$-dimensional space-times, this is mainly due to that a gravitational potential proportional to $\sim 1/r$ only in $3+1$-dimensional space-times corresponds to a finite gravitational mass. Also we note that such a divergence near the singularity is usually associated with a breakdown of the theory such that a more complete theory is required. A simple regularization for the divergent quantities is to consider a lower cut-off δ_{IR} of the order of the Planck length near the singularity as was considered in [23].

As for configurations for which the total mass M, the total angular momentum J_z and the total magnetic flux $\Phi_{\mathcal{B}}$ are divergence when the integral of the respective densities is considered up to spatial infinity, let us note that considering a upper cut-off δ_{UV} for large values of the radial coordinate r is simply interpreted as a description of a finite size system such that the cut-off δ_{UV} is interpreted as the maximum size of the system. Otherwise, for infinite size systems, it is not mandatory that these quantities be finite, instead they may be interpreted as cosmological-like solutions for $2+1$-dimensional space-times as long as the respective densities are finite away from the singularity at the origin. Let us note that even for a uniformly distributed (meaning constant) mass-energy density in flat Minkowski space-time we would obtain a divergent total mass when integrating over all space up to spatial infinity.

Hence for the classical configurations discussed here, to regularize the divergence at the origin for M, S_z or $\Phi_{\mathcal{B}}$ we consider the lower cut-off δ_{IR} to be of the order of the Planck length l_p. To interpret the divergence and the respective upper cut-off δ_{UV} for large r let us consider three possible cases:

- *string-like configurations*: a $2+1$-dimensional point-like effective description of matter centered at the origin generating a magnetic field of finite flux. When embedded into a $3+1$-dimensional space-time with cylindrical symmetry is interpreted as a magnetic string configuration. These configurations should also have a finite mass and finite angular momentum such that the upper cut-off δ_{UV} is not required;

- *configurations driven by an external magnetic field*: the upper cut-off δ_{UV} is justified by the finite range of the applied external field. Hence, from the point of view of $3+1$-dimensions the magnetic field has cylindrical symmetric and is applied orthogonally to the planar system in the region $r < \delta_{UV}$;

- *cosmological-like solutions*: an infinite configuration with background magnetic fields such that are allowed total infinite magnetic flux, infinite mass and angular momentum as long as the respective densities are (locally) finite everywhere except at the space-time singularities.

By inspection of the table 1 we conclude that, considering only the cut-off δ_{IR} the solutions with a magnetic field generating a finite total flux, hence being interpreted as a magnetic string-like configuration in an infinite space-time are achievable only for the parameter range $p \in]-\infty, -1[$ corresponding to solution III describing ghost gauge fields. For these configurations also the total mass and total angular momentum are finite. We remark that due to the particular value of the parameter $p = -1$ not allowing for a solution of the equations of motion, this configurations cannot be obtained from flat Minkowski space-time by continuously changing the parameter p.

As for the range $p \in]-1, 1[$ (considering the lower cut-off δ_{IR}), M and J_z are finite. However, although the magnetic field $\mathcal{B}$ is finite, the total magnetic flux $\Phi_{\mathcal{B}}$ is divergent when integrating the magnetic field up to spatial infinity, hence these solutions can be interpreted either as driven by a cylindrical external magnetic field orthogonal to the planar system ranging from the origin up to the upper cut-off $r < \delta_{UV}$, either as a cosmological-like solution. In addition we note that, when considering an external magnetic field, the value of the field $\mathcal{B}$ is null for $p = 0$ and $p = 1/2$. Hence the solutions corresponding to these values of the parameters are interpreted as two possible backgrounds upon which the external magnetic field is applied to. Specifically $p = 0$ corresponds to empty flat Minkowski, such that when the magnetic field is turn on the solutions can be changed smoothly and continuously by varying the parameter p (the variation of the field solutions with the parameter p are continuous and their derivatives with respect to p are also continuous) describing the deformation induced by the magnetic field, in the range $p \in]-1/4, 0[$ corresponding to solution III (2.8) for ghost gauge fields, in the range $p \in]0, 1/2[$ also for ghost gauge fields corresponding to solution I and in the range $p \in]0, 1/3[$ for standard gauge fields corresponding to solution II. For $p = 1/2$ the background corresponds to a neutral dilatonic-like background and the solutions can be changed smoothly and continuously by varying the parameter p in the range $p \in]0, 1/2[$ describing ghost gauge fields corresponding to solution I and in the range $p \in]1/2, 2/3]$ describing standard gauge fields corresponding to solution II. In the range $p \in [2/3, 1[$ corresponding to solution IV describing standard gauge fields the solutions can also be changed smoothly and continuously by varying the parameter p, however when crossing the value $p = 2/3$ the derivative of the field solutions is not continuous such that this range cannot be obtained smoothly by varying the value of the parameter p starting at any of the neutral backgrounds $p = 0$ or $p = 1/2$.

For values of the parameter $p \in [1, 3/2]$ corresponding to solution IV describing standard gauge fields the metric ADM signature for values of the radial coordinate above the value of the radial coordinate of the horizon, $r > r_H$, is the opposite to our original convention, while for the range $r \in]0, r_H[$ the metric has the ADM signature $\mathrm{diag}(-,+,+)$ corresponding to the original convention. The interpretation for an external observer is that observable space-time is between $r = 0$ and the coordinate horizon $r = r_H$ (2.28) such that $r = 0$ is a dressed singularity ($r = 0$ is both a singularity and an horizon) and a cosmological horizon exists at $r = r_H$. In addition we note that the geodesics divergence analyzed in section 2.3 located at $r = r_{\mathrm{div}}$ (2.26), is now beyond the cosmological horizon, specifically for $p > 1$ we obtain that $r_H < r_{\mathrm{div}}$. These configurations may be interpreted as cosmological-like configurations in $2+1$-dimensions as the mass-energy density, the magnetic field and pressure are finite in between horizons.

As for the range $p \in]3/2, +\infty[$ we obtain an exotic configuration for which space-time has two singularities at $r = 0$ and $r = +\infty$. In particular for the range $p \in]2, +\infty[$, M, S_z and $\Phi_{\mathcal{B}}$ have no divergence at the origin having only a divergence at spatial infinity. Hence by considering the map $\hat{r} = 1/r$ we obtain, for our metric ADM signature convention, a magnetic string-like configuration for standard gauge fields with both a singularity at the origin within the horizon at $\hat{r}_H > \hat{r}_{\mathrm{div}}$ and a dressed singularity at spatial infinity (spatial infinity is itself both a singularity and an horizon).

We resume the main configuration types discussed in table 2.

configuration type	p	solution
string-like	$\in \,]-\infty, -1[$	III (ghost)
driven by B_*	$\in \left]-1, \frac{1}{2}\right]$	I(ghost) and III(ghost) $p = 0 \Leftrightarrow$ neutral background
	$\in \left[0, \frac{1}{2}\right[$	II $p = 0 \Leftrightarrow$ neutral background
	$\in \left[\frac{1}{2}, \frac{2}{3}\right]$	II $p = \frac{1}{2} \Leftrightarrow$ neutral background
cosmological-like	$\in \left]\frac{2}{3}, \frac{3}{2}\right]$	IV

Tabela 2: Resume of discussed configuration types.

As a final remark we note that the magnetic string-like configuration corresponding to solution III for the range of the parameter $p \in]-\infty, -1[$ describing a ghost gauge sector suggests that, for extended gauge theories containing a ghost gauge sector coupled to magnetic charge [60, 61], similar magnetically charged solutions may be computed in $3+1$-dimensions [62] and $2+1$-dimensions [63].

Acknowledgments

This work was supported by Grant SFRH/BPD/34566/2007 up to January 2014 and by project CENTRO-01-0145-FEDER-000014 from August 2017 onwards.

A Magnetic Solutions

For completeness, in this appendix we re-derive, directly from the equations of motion for action (2.1) in the Cartan-frame, the solutions (2.5) obtained in the main text from space-time duality. In form notation the action (2.1) is

$$\begin{aligned} S &= -\int_M \left\{ e^{a\phi} \left[\tilde{R} * 1 + 2\lambda\, d\phi \wedge *d\phi \right] - e^{b\phi} \Lambda * 1 \right. \\ &\quad \left. + \hat{\epsilon} e^{c\phi} \left[\tilde{F} \wedge *\tilde{F} + *J \wedge \tilde{A} \right] + \hat{\epsilon} \frac{m}{2}\, \tilde{A} \wedge \tilde{F} \right\} \end{aligned}$$

using the metric parameterization (2.2)

$$d\tilde{s}^2 = -\tilde{f}^2 (dt + \tilde{A} d\varphi)^2 + dr^2 + \tilde{h}^2 d\varphi^2 \ .$$

The Cartan triad is then given by

$$\begin{aligned} e^0 = d\theta^0 &= \tilde{f}(dt + \tilde{A}d\varphi) \,, \\ e^1 = d\theta^1 &= dr \,, \\ e^2 = d\theta^2 &= \tilde{h}d\varphi \,, \\ e^0{}_0 = \tilde{f} \,, \quad e^0{}_1 = 0 \,, \quad e^0{}_2 &= \tilde{f}\tilde{A} \,, \\ e^1{}_0 = 0 \,, \quad e^1{}_1 = 1 \,, \quad e^1{}_2 &= 0 \,, \\ e^2{}_0 = 0 \,, \quad e^2{}_1 = 0 \,, \quad e^2{}_2 &= \tilde{h} \,, \end{aligned} \tag{A.1}$$

such that the line element in the Cartan-frame is

$$d\tilde{s}^2 = e^i e_i = \eta_{ij} d\theta^i d\theta^j = -(d\theta^0)^2 + (d\theta^1)^2 + (d\theta^2)^2 \,, \tag{A.2}$$

The electric field $\tilde{E}_*$ and magnetic field $\tilde{B}_*$ in the coordinate frame are given by

$$\begin{aligned} \tilde{E}_* &= \tilde{E}\,\tilde{f} \,, \\ \tilde{B}_* &= \tilde{B}\,\tilde{h} - \tilde{E}\,\tilde{f}\,\tilde{A} \,, \end{aligned} \tag{A.3}$$

where $\tilde{E}$ and $\tilde{E}$ are the electromagnetic fields in the Cartan-frame. We note that the metric parameterization (2.2) allows for the electric field to be null both in the coordinate frame and in the Cartan-frame, $\tilde{E} = 0 \Leftrightarrow \tilde{E}_* = 0$. This parameterization also allows for the Maxwell equations in the Cartan-frame to have purely magnetic solutions as we will derive next.

Noting that

$$\begin{aligned} de^0 &= -\beta e^0 \wedge e^1 + \gamma e^1 \wedge e^2 \,, \\ de^2 &= \alpha e^1 \wedge e^2 \,, \end{aligned} \tag{A.4}$$

the Equations of motion, connections, curvature and remaining quantities depend only on the combinations

$$\alpha = \frac{\tilde{h}'}{\tilde{h}} \,, \quad \beta = \frac{\tilde{f}'}{\tilde{f}} \,, \quad \gamma = \frac{\tilde{f}\,\tilde{A}'}{\tilde{h}} \,. \tag{A.5}$$

The non null connections in the Cartan-frame are

$$\begin{aligned} &\omega^0{}_{10} = \omega^1{}_{00} = \beta \,, \\ &\omega^0{}_{12} = \omega^1{}_{02} = \omega^1{}_{20} = -\omega^0{}_{21} = -\omega^2{}_{01} = -\omega^2{}_{10} = \gamma/2 \,, \\ &\omega^1{}_{22} = -\omega^2{}_{12} = -\alpha \,, \end{aligned} \tag{A.6}$$

and the Einstein and the energy-momentum tensor components are

$$\begin{aligned} \tilde{G}_{00} &= -\alpha^2 + 3\gamma^2/4 - \alpha' \,, \\ \tilde{G}_{11} &= \alpha\beta + \gamma^2/4 \,, \\ \tilde{G}_{22} &= \beta^2 + \gamma^2/4 + \beta' \,, \\ \tilde{G}_{02} &= \beta\gamma + \gamma'/2 \,, \\ 2\tilde{T}_{00} &= \hat{\epsilon}\left(\tilde{B}^2 + \tilde{E}^2\right) \,, \\ 2\tilde{T}_{11} &= \hat{\epsilon}\left(\tilde{B}^2 - \tilde{E}^2\right) \,, \\ 2\tilde{T}_{22} &= \hat{\epsilon}\left(\tilde{B}^2 + \tilde{E}^2\right) \,, \\ 2\tilde{T}_{02} &= -2\hat{\epsilon}\tilde{B}\tilde{E} \,, \\ \Phi_{00} &= -a\phi'' + (\lambda/2 - a^2)(\phi')^2 \,, \\ \Phi_{11} &= \lambda/2(\phi')^2 \,, \\ \Phi_{22} &= a\phi'' - (\lambda/2 - a^2)(\phi')^2 \,. \end{aligned} \tag{A.7}$$

We note that under the duality (1.3) only the dilaton contribution to the energy-momentum tensor is invariant while the Maxwell energy-momentum tensor acquires a minus sign (this accounts to take $\hat{\epsilon} \to -\hat{\epsilon}$) and for the Einstein tensor the terms $\gamma^2/4$ and $3\gamma^2/4$ are swapped. For a direct comparison with the same tensor quantities for the standard metric ADM parameterization (1.1) we refer the reader to the appendix of [23]). In the following we consider both cases $\hat{\epsilon} = +1$ and $\hat{\epsilon} = -1$.

The Maxwell Equations are

$$\tilde{B}' + \beta\tilde{B} + c\,\tilde{B}\,\phi' = m\,\tilde{E}\,e^{-c\phi} \,, \tag{A.8}$$

$$\tilde{E}' + \alpha\tilde{E} + c\,\tilde{E}\,\phi' + \gamma\tilde{B} = -m\,\tilde{B}\,e^{-c\phi} \,, \tag{A.9}$$

for purely magnetic solutions $\tilde{E} = \tilde{E}* = 0$ the Einstein equations are

$$e^{a\phi}\left(\beta\gamma + \frac{\gamma'}{2}\right) = 0 \,, \tag{A.10}$$

$$e^{a\phi}\left[\alpha^2 - \frac{3\gamma^2}{4} + \alpha' + a\phi'' + \left(a^2 - \frac{\lambda}{2}\right)(\phi')^2\right] + \frac{1}{2}e^{b\phi}\Lambda = \hat{\epsilon}\tilde{B}^2 e^{c\phi} \,, \tag{A.11}$$

$$e^{a\phi}\left[\beta^2 + \frac{\gamma^2}{4} + \beta' + a\phi'' + \left(a^2 - \frac{\lambda}{2}\right)(\phi')^2\right] + \frac{1}{2}e^{b\phi}\Lambda = -\hat{\epsilon}\tilde{B}^2 e^{c\phi} \,, \tag{A.12}$$

$$e^{a\phi}\left[\alpha\beta + \frac{\gamma^2}{4} + \frac{\lambda}{2}(\phi')^2\right] + \frac{1}{2}e^{b\phi}\Lambda = -\hat{\epsilon}\tilde{B}^2 e^{c\phi} \,, \tag{A.13}$$

and the Dilaton equation is

$$e^{a\phi}\left[(4a^2-\lambda)\phi''+a\left(4a^2-2\lambda\right)(\phi')^2\right]+ +(3a-b)e^{b\phi}\Lambda=-\hat{\epsilon}(a+c)\tilde{B}^2e^{c\phi}\,. \tag{A.14}$$

From the second Maxwell Equation (A.9) we obtain

$$\gamma=-m\,e^{-c\phi}\,. \tag{A.15}$$

Using (A.15) in (A.10) one obtains that $\beta=c\phi'/2$ such that

$$\tilde{f}=c_f\,e^{\frac{c}{2}\phi}\,, \tag{A.16}$$

where c_f is a free integration constant. From the first Maxwell Equation (A.8) with $\tilde{E}=0$ we obtain

$$\tilde{B}=\chi e^{-\frac{3}{2}c\phi}\,, \tag{A.17}$$

where χ is an integration constant. The remain 3 Einstein (A.11), (A.12), (A.13) and the dilaton equation (A.14) are

$$a\phi''+(a^2-\frac{\lambda}{2})(\phi')^2+\alpha^2+\alpha'-\frac{3m^2}{4}e^{-2c\phi}+\frac{1}{2}\Lambda e^{(b-a)\phi} = \hat{\epsilon}\chi^2e^{(-a-2c)\phi}\,, \tag{A.18}$$

$$(a+\frac{c}{2})\phi''+(a^2-\frac{\lambda}{2}+\frac{c^2}{4})(\phi')^2+\frac{m^2}{4}e^{-2c\phi}+\frac{1}{2}\Lambda e^{(b-a)\phi} = -\hat{\epsilon}\chi^2e^{(-a-2c)\phi}\,, \tag{A.19}$$

$$\frac{\lambda}{2}(\phi')^2+\frac{c}{2}\alpha\phi'+\frac{m^2}{4}e^{-2c\phi}+\frac{1}{2}\Lambda e^{(b-a)\phi} = -\hat{\epsilon}\chi^2e^{(-a-2c)\phi}\,, \tag{A.20}$$

$$(4a^2-\lambda)\phi''+a(4a^2-2\lambda)(\phi')^2+(3a-b)\Lambda e^{(b-a)\phi} = -\hat{\epsilon}(a+c)\chi^2e^{(-a-2c)\phi}\,. \tag{A.21}$$

Employing the same ansatz of [23]

$$\begin{aligned} a &= 0\,,\\ c &= -\frac{b}{2}\,,\\ \lambda &\neq \frac{b^2}{8}\,, \end{aligned} \tag{A.22}$$

where the particular case corresponding to $b^2=8\lambda$ is excluded due to not admitting a solution for the above equations of motion. Given this ansatz we combine (A.19) with (A.21) obtaining

$$\phi'=\pm\sqrt{c_1}e^{\frac{b}{2}\phi}\,, \tag{A.23}$$

such that the Dilaton is

$$\phi=-\frac{2}{b}\ln(c_\phi\,r)\,, \tag{A.24}$$

where

$$\begin{aligned} c_\phi &= \frac{|b|}{2}\sqrt{c_1}\,,\\ c_1 &= -2\frac{b^2(\hat{\epsilon}\chi^2+2\Lambda)+2\lambda(4\hat{\epsilon}\chi^2+2\Lambda+m^2)}{\lambda(b^2-8\lambda)}\,. \end{aligned} \tag{A.25}$$

Imposing either of the equations (A.19) or (A.21) to be obeyed by this solution we obtain that

$$\chi^2=-\hat{\epsilon}\frac{2\Lambda(b^2+12\lambda)+4\lambda m^2}{b^2+24\lambda}\,, \tag{A.26}$$

such that c_1 is rewritten as

$$c_1=4\,\frac{m^2-6\Lambda}{b^2+24\lambda}\,, \tag{A.27}$$

and from (A.20) we obtain

$$\alpha=-\left(16\frac{\lambda}{b^2}+1\right)\frac{1}{2\,r}\,. \tag{A.28}$$

Therefore

$$\tilde{h}=c_h\,r^{-\frac{8\lambda}{b^2}-\frac{1}{2}}\,, \tag{A.29}$$

and from (A.16)

$$\tilde{f}=c_f\,\sqrt{r}\,, \tag{A.30}$$

where c_h and c_f are free constants. From (A.15) we obtain that

$$\tilde{A}=c_A\,r^{-\frac{8\lambda}{b^2}-1}+c_{A_\infty}\,, \tag{A.31}$$

where

$$c_A=\frac{m\,C_h}{C_f\left(\frac{8\lambda}{b^2}+1\right)}\sqrt{\frac{1+\frac{24\lambda}{b^2}}{m^2-6\Lambda}}\,. \tag{A.32}$$

Replacing these solutions in (A.18) and demanding this equation to be obeyed we obtain that

$$\lambda_\pm=\frac{b^2}{8}\,\frac{3\Lambda\mp\sqrt{\Lambda(2m^2-3\Lambda)}}{m^2-6\Lambda}\,. \tag{A.33}$$

It is further required to ensure that all these relations are possible for real valued constants, in particular that $c_1>0$ and $\chi^2>0$. We note that the condition $c_1>0$ is obeyed in the range $0<\Lambda<m^2/3$ except for the particular case $\Lambda=m^2/6$ for which $c_1=0$. Then, imposing the

condition $\chi^2 > 0$, we obtain the four possible solutions and respective bounds on the cosmological constant

$$\left\{\begin{array}{l}\hat\epsilon=+1\\ \lambda=\lambda_+\end{array}\right. : \left\{\begin{array}{l}\chi^2=\frac{1}{2}\left[-\Lambda+\sqrt{\Lambda(2m^2-3\Lambda)}\right]\\ c_1=\frac{4}{b^2}\left[3\Lambda+m^2+\sqrt{\Lambda(2m^2-3\Lambda)}\right]\\ \qquad 0<\Lambda<\frac{m^2}{2}\end{array}\right.$$

$$\left\{\begin{array}{l}\hat\epsilon=-1\\ \lambda=\lambda_+\end{array}\right. : \left\{\begin{array}{l}\chi^2=\frac{1}{2}\left[\Lambda-\sqrt{\Lambda(2m^2-3\Lambda)}\right]\\ c_1=\frac{4}{b^2}\left[3\Lambda+m^2+\sqrt{\Lambda(2m^2-3\Lambda)}\right]\\ \qquad 0<\Lambda<\frac{m^2}{6}\ \vee\ \frac{m^2}{2}<\Lambda<\frac{2m^2}{3}\end{array}\right.$$

$$\left\{\begin{array}{l}\hat\epsilon=+1\\ \lambda=\lambda_-\end{array}\right. : \left\{\begin{array}{l}\chi^2=\frac{1}{2}\left[\Lambda+\sqrt{\Lambda(2m^2-3\Lambda)}\right]\\ c_1=\frac{4}{b^2}\left[3\Lambda+m^2-\sqrt{\Lambda(2m^2-3\Lambda)}\right]\\ \qquad 0<\Lambda<\frac{m^2}{6}\end{array}\right.$$

$$\left\{\begin{array}{l}\hat\epsilon=-1\\ \lambda=\lambda_-\end{array}\right. : \left\{\begin{array}{l}\chi^2=\frac{1}{2}\left[\Lambda+\sqrt{\Lambda(2m^2-3\Lambda)}\right]\\ c_1=\frac{4}{b^2}\left[3\Lambda+m^2-\sqrt{\Lambda(2m^2-3\Lambda)}\right]\\ \qquad \frac{m^2}{6}<\Lambda<\frac{2m^2}{3}\end{array}\right. \tag{A.34}$$

B Expressions for M, S_z and $\Phi_{\mathcal{B}}$ for particular values of the parameter p

In this appendix are listed the explicit expressions for the mass M (2.35), angular momentum S_z (2.36) and magnetic flux $\Phi_{\mathcal{B}}$ (2.41) for the particular values of the parameter p not included in the expressions (2.37), (2.39) and (2.42).

Evaluating the integral expression for the mass M for $p=1$ with A given in (2.9) we obtain

$$\begin{aligned} p &= 1\,,\\ M &= -\frac{\hat\epsilon C_B^2 C_\phi \pi}{|C_f C_h|}\Big(r^{-1}\Big(1-\tilde C_A^2-(\tilde C_A+\tilde\theta)\times\\ &\quad\times(\tilde C_A+\tilde\theta+2\tilde C_A\,\log(r))-\tilde C_A^2\,\log(r)^2\Big)\Big)_{r=\delta_{IR}}\,, \end{aligned} \tag{B.1}$$

for $p=6/5$ evaluating (2.35) we obtain

$$\begin{aligned} p &= \frac{6}{5}\,,\\ M &= \frac{\hat\epsilon C_B^2 C_\phi \pi}{|C_f C_h|}\Bigg(-\frac{5}{4}r^{-\frac{4}{5}}\left(8\tilde C_A\tilde\theta\,r^{\frac{3}{5}}+2\tilde\theta^2\,r^{\frac{2}{5}}-1\right)\\ &\quad+\tilde C_A^2\log(r)\Bigg)_{\delta_{IR}}^{\delta_{UV}}\,, \end{aligned} \tag{B.2}$$

for $p=4/3$ we obtain

$$\begin{aligned} p &= \frac{4}{3}\,,\\ M &= \frac{\hat\epsilon C_B^2 C_\phi \pi}{2|C_f C_h|}\Bigg(3r^{-\frac{2}{3}}\left(\tilde C_A^2\,r^{\frac{4}{3}}+4\tilde C_A\tilde\theta\,r+1\right)\\ &\quad+2\tilde\theta^2\log(r)\Bigg)_{\delta_{IR}}^{\delta_{UV}}\,, \end{aligned} \tag{B.3}$$

for $p=5/4$ we obtain

$$\begin{aligned} p &= \frac{5}{4}\,,\\ M &= \frac{2\hat\epsilon C_B^2 C_\phi \pi}{3|C_f C_h|}\Bigg(r^{-\frac{3}{4}}\left(6\tilde C_A^2\,r-6\tilde\theta^2\,r^{\frac{1}{2}}+2\right)\\ &\quad+3\tilde C_A\tilde\theta\log(r)\Bigg)_{\delta_{IR}}^{\delta_{UV}}\,, \end{aligned} \tag{B.4}$$

and for $p=2$ we obtain

$$\begin{aligned} p &= 2\\ M &= \frac{\hat\epsilon C_B^2 C_\phi \pi}{12|C_f C_h|}\Bigg(r^2\left(3\tilde C_A^2\,r^2+8\tilde C_A\tilde\theta\,r+6\tilde\theta^2\right)\\ &\quad-12\log(r)\Bigg)_{\delta_{IR}}^{\delta_{UV}}\,. \end{aligned} \tag{B.5}$$

Evaluating the integral expression for the angular momentum S_z for $p = 1$ with A given in (2.9) we obtain

$$\begin{aligned} p &= 1\,, \\ S_z &= +\frac{\hat{\epsilon} C_B^2 C_\phi \pi}{(C_f C_h)^2}\Bigg(r^{-1}\,\Big((\tilde{C}_A+\tilde{\theta})^2+\tilde{C}_A(5\tilde{C}_A+3\tilde{\theta}) \\ &\quad -\tilde{\theta}+\tilde{C}_A\log(r)\,\Big(3(\tilde{C}_A+\tilde{\theta})^2+3\tilde{C}_A-1 \\ &\quad +\tilde{C}_A\log(r)(3(\tilde{C}_A+\tilde{\theta})+\tilde{C}_A\log(r))\Big)\Big)\Bigg)_{r=\delta_{IR}}\,, \end{aligned} \tag{B.6}$$

for $p = 7/6$ evaluating (2.36) we obtain

$$\begin{aligned} p &= \frac{7}{6}\,, \\ S_z &= \frac{\hat{\epsilon} C_B^2 C_\phi \pi}{(C_f C_h)^2}\Bigg(-18\tilde{C}_A^2\tilde{\theta} r^{-\frac{1}{6}}-9\tilde{C}_A\tilde{\theta}^2\,r^{-\frac{1}{3}}-2\tilde{\theta}^3\,r^{-\frac{1}{2}} \\ &\quad +\frac{3}{2}\tilde{C}_A\,r^{-\frac{2}{3}}+\frac{6}{5}\tilde{\theta}\,r^{-\frac{5}{6}}+\tilde{C}_A^3\log(r)\Bigg)_{\delta_{IR}}^{\delta_{UV}}\,, \end{aligned} \tag{B.7}$$

for $p = 6/5$ we obtain

$$\begin{aligned} p &= \frac{6}{5}\,, \\ S_z &= \frac{5\hat{\epsilon} C_B^2 C_\phi \pi}{12(C_f C_h)^2}\Bigg(12\tilde{C}_A^3\,r^{\frac{1}{5}}-36\tilde{C}_A\tilde{\theta}^2\,r^{-\frac{1}{5}}+4\tilde{C}_A\,r^{-\frac{3}{5}} \\ &\quad +3\tilde{\theta}\,r^{-\frac{4}{5}}-6\tilde{\theta}^3\,r^{-\frac{2}{5}}+\frac{36}{5}\tilde{C}_A^2\tilde{\theta}\log(r)\Bigg)_{\delta_{IR}}^{\delta_{UV}}\,, \end{aligned} \tag{B.8}$$

for $p = 5/4$ we obtain

$$\begin{aligned} p &= \frac{5}{4}\,, \\ S_z &= \frac{\hat{\epsilon} C_B^2 C_\phi \pi}{3(C_f C_h)^2}\Bigg(6\tilde{C}_A^3\,r^{\frac{1}{2}}+6\tilde{C}_A\,r^{-\frac{1}{2}}+4\tilde{\theta}\,r^{-\frac{3}{4}} \\ &\quad -12\tilde{\theta}^3\,r^{-\frac{1}{4}}+36\tilde{C}_A^2\tilde{\theta}\,r^{\frac{1}{4}}+9\tilde{C}_A\tilde{\theta}^2\log(r)\Bigg)_{\delta_{IR}}^{\delta_{UV}}\,, \end{aligned} \tag{B.9}$$

and for $p = 4/3$ we obtain

$$\begin{aligned} p &= \frac{4}{3}\,, \\ S_z &= \frac{\hat{\epsilon} C_B^2 C_\phi \pi}{2(C_f C_h)^2}\Bigg(2\tilde{C}_A^3\,r+18\tilde{C}_A\tilde{\theta}^2\,r^{\frac{1}{3}}+6\tilde{C}_A\,r^{-\frac{1}{3}} \\ &\quad +3\tilde{\theta}\,r^{-\frac{2}{3}}+9\tilde{C}_A^2\tilde{\theta} r^{\frac{2}{3}}+2\tilde{\theta}^3\log(r)\Bigg)_{\delta_{IR}}^{\delta_{UV}}\,, \end{aligned} \tag{B.10}$$

for $p = 3/2$ we obtain

$$\begin{aligned} p &= \frac{3}{2}\,, \\ S_z &= \frac{\hat{\epsilon} C_B^2 C_\phi \pi}{(C_f C_h)^2}\Bigg(\frac{1}{2}\tilde{C}_A^3\,r^2+3\tilde{C}_A\tilde{\theta}^2\,r+2\tilde{\theta}\,r^{-\frac{1}{2}} \\ &\quad +2\tilde{\theta}^3\,r^{\frac{1}{2}}+2\tilde{C}_A^2\tilde{\theta}\,r^{\frac{3}{2}}-\tilde{C}_A\log(r)\Bigg)_{\delta_{IR}}^{\delta_{UV}}\,, \end{aligned} \tag{B.11}$$

for $p = 2$ we obtain

$$\begin{aligned} p &= 2\,, \\ S_z &= \frac{\hat{\epsilon} C_B^2 C_\phi \pi}{20(C_f C_h)^2}\Bigg(4\tilde{C}_A^3\,r^5+20\tilde{C}_A\tilde{\theta}^2\,r^3-20\tilde{C}_A\,r \\ &\quad +10\tilde{\theta}^3\,r^2+15\tilde{C}_A^2\tilde{\theta}\,r^4-20\tilde{\theta}\log(r)\Bigg)_{\delta_{IR}}^{\delta_{UV}}\,. \end{aligned} \tag{B.12}$$

Evaluating the integral expression for the magnetic flux $\Phi_{\mathcal{B}}$ for $p = 1$ with A given in (2.9) we obtain

$$\begin{aligned} p &= 1\,, \\ \Phi_{\mathcal{B}} &= \frac{2C_B^2 C_h^2 C_\phi \pi}{27}\,\Big(r^3\,\Big(9-2\tilde{C}_A^2+6\tilde{C}_A\tilde{\theta}-9\tilde{\theta}^2 \\ &\quad +3\tilde{C}_A\log(r)\,\Big(2\tilde{C}_A-6\tilde{\theta}-3\tilde{C}_A\log(r)\Big)\Big)\Big)_{r=\delta_{UV}}\,, \end{aligned} \tag{B.13}$$

for $p = 1/3$ evaluating (2.41) we obtain

$$\begin{aligned} p &= \frac{1}{3}\,, \\ \Phi_{\mathcal{B}} &= -C_B C_\phi C_h^2\pi\Bigg(-\frac{3}{2}\,r^{\frac{4}{3}}-6\tilde{\theta}\tilde{C}_A\,r^{-\frac{2}{3}} \\ &\quad -\frac{3}{2}\tilde{C}_A^2\,r^{\frac{4}{3}}+2\tilde{\theta}^2\log(r)\Bigg)_{\delta_{IR}}^{\delta_{UV}}\,, \end{aligned} \tag{B.14}$$

and for $p = 3/5$ we obtain

$$\begin{aligned} p &= \frac{3}{5}\,, \\ \Phi_{\mathcal{B}} &= -C_B C_\phi C_h^2\pi\Bigg(-\frac{5}{4}\,r^{\frac{8}{5}}+\frac{5}{2}\tilde{\theta}^2\,r^{\frac{4}{5}} \\ &\quad +10\tilde{\theta}\tilde{C}_A\,r^{\frac{2}{5}}+2\tilde{C}_A^2\log(r)\Bigg)_{\delta_{IR}}^{\delta_{UV}}\,. \end{aligned} \tag{B.15}$$

Referências

[1] S. Deser, R. Jackiw and G. 't Hooft, *Three-Dimensional Einstein Gravity: Dynamics of Flat Space*, Annals Phys. **152** (1984) 220-235 .

[2] S. Deser and R. Jackiw, *Three-dimensional cosmological gravity: Dynamics of constant curvature*, Annals Phys. **153** (1984) 405-416 .

[3] M. Bañados, C. Teitelboim and J. Zanelli, *The Black Hole in Three-Dimensional Space-Time*, Phys.Rev. Lett. **69** (1992) 1849-1851, hep-th/9204099.

[4] I. I. Kogan, *About Some Exact Solutions for $2+1$ Gravity Coupled to Gauge Fields*, Mod. Phys. Lett. **A7** (1992) 2341-2350, hep-th/9205095.

[5] I. I. Kogan, *Black Hole Spectrum, Horizon Quantization and All That*, hep-th/9412232.

[6] C. Martinéz, M. Henneaux, C. Teitelboim and J. Zanelli, *Geometry of the (2+1) Black Hole*, Phys. Rev. **D48** (1993) 1506-1525, gr-qc/9302012 .

[7] S. Carlip, *The (2+1)-dimensional Black Hole*, Class. Quant. Grav. **12** (1995) 2853-2880, gr-qc/9506079.

[8] G. Clément, *Classical Solutions In Three-Dimensional Einstein-Maxwell Cosmological Gravity*, Class. Quant. Grav. **10** (1993) L49-L54.

[9] G. Clément, *Classical Solutions of Gravitating Chern-Simons Electrodynamics*, gr-qc/9406052.

[10] S. Fernando and F. Mansouri, *Rotating Charged Solutions to Einstein-Maxwell-ChernSimons Theory in $2+1$ Dimensions*, Comm. Math. Theor. Phys. **1** (1998) 14, gr-qc/9705016.

[11] T. Dereli and Y. N. Obukhov, *General Analysis of Self-Dual Solutions for the Einstein-Maxwell-Chern-Simons Theory in $(1+2)$ Dimensions*, gr-qc/0001017.

[12] T. Andrade, M. Bañados, R. Benguria and A. Gomberoff, *The $2+1$ Charged Black Hole in Topologically Massive Electrodynamics*, hep-th/0503095.

[13] C. Martinéz, C. Teitelboim and J. Zanelli, *Charged Rotating Black Hole in Three Space-Time Dimensions*, Phys.Rev. **D61** (2000) 104013, hep-th/9912259.

[14] J. P. S. Lemos, *Cylindrical Black Hole in General Relativity*, Phys. Lett. **B353** (1995) 46-51, gr-qc/9404041.

[15] K. C. K. Chan and R. B. Mann, *Static Charged Black Holes in (2+1)-dimensional Dilaton Gravity*, Phys. Rev. **D50** (1994) 6385, gr-qc/9404040; Erratum-ibid. **D52** (1995) 2600 .

[16] K. C. K. Chan and R. B. Mann, *Spinning Black Holes in (2+1)-Dimensional String and Dilaton Gravity*, Phys. Lett. **B371** (1996) 199-205, gr-qc/9510069.

[17] P. M. Sá, A. Kleber and J. P. S. Lemos, *Black Holes in Three-Dimensional Dilaton Gravity Theories*, Class. Quant. Grav. **13** (1996) 125-138, hep-th/9503089.

[18] O. J. C. Dias and J. P. S. Lemos, *Rotating Magnetic Solution in Three-Dimensional Einstein Gravity*, JHEP (2002) 0201:006, hep-th/0201058.

[19] O. J. C. Dias and J. P. S. Lemos, *Magnetic Point Sources in Three Dimensional Brans-Dicke Gravity Theories*, Phys. Rev. **D66** (2002) 024034, hep-th/0206085.

[20] O. J. C. Dias and J. P. S. Lemos, *Magnetic Strings in Anti-de Sitter General Gravity*, Class. Quant. Grav. **19** (2002) 2265-2276, hep-th/0110202.

[21] O. J. C. Dias and J. P. S. Lemos, *Static and Rotating Electrically Charged Black Holes in Three-Dimensional Brans-Dicke Gravity Theories*, Phys. Rev. **D64** (2001) 064001, hep-th/0105183.

[22] O. J. C. Dias, *Black Hole Solutions and pair creation of Black Holes in three, Four and Higher Dimensional SpaceTimes*, Ph.D Thesis, hep-th/0410294.

[23] P. Castelo Ferreira, *Rotating Electric Classical Solutions of $2+1$ D $U(1)$ Einstein Maxwell Chern-Simons*, Class. Quant. Grav. **23** (2006) 3679-3706, hep-th/0506244.

[24] G. Clément, *Particle-Like Solutions to Topologically Massive Gravity*, Class. Quant. Grav. **11** (1994) L115-L120, gr-qc/9404004.

[25] K. A. Moussa, G. Clément, *Topologically Massive Gravito Electrodynamics: Exact Solutions*, Class. Quant. Grav. **13** (1996) 2319-2328, gr-qc/9602034.

[26] A Ferstl, B. Tekin and V. Weir, *Gravitating Instantons in Three-Dimensional Anti-De Sitter Space*, Phys. Rev. **D62** (2000) 064003, hep-th/0002019.

[27] G. Clément, *Black Hole Mass and Angular Momentum in $2+1$ Gravity*, Phys. Rev. **D68** (2003) 024032, gr-qc/0301129.

[28] K. A. Moussa, G. Clément and C. Leygnac, *The Black Holes of Topologically Massive Gravity*,Class. Quant. Grav. **20** (2003) L277-L283, gr-qc/0303042.

[29] S. Deser and B. Tekin, *Energy in Topologically Massive Gravity*, Class. Quant. Grav. **20** (2003) L259, gr-qc/0307073.

[30] C. Nazaroglu, Y. Nutku, B. Tekin, *Covariant Symplectic Structure and Conserved Charges of Topologically Massive Gravity*, Phys. Rev. **D 83** (2011) 124039 , arXiv:1104.3404.

[31] C. Martínez, R. Troncoso and J. Zanelli, *Exact Black Hole Solution with a Minimally Coupled Scalar Field*, Phys. Rev., **D70** (2004) 084035, `hep-th/0406111`.

[32] S. Chandrasekhar, *Cylindrical Waves in General Relativity*, Proc. Roy. Soc. Lond. **A408** (1986) 209-232.

[33] J. P. S. Lemos, *Cylindrical Black Hole in General Relativity*, Phys. Lett. **B353** (1995) 46-51, `gr-qc/9404041`.

[34] S. Deser, R. Jackiw and S. Templeton, *Three-Dimensional Massive Gauge Theories*, Phys.Rev. Lett. **48** (1982) 975.

[35] S. Deser, R. Jackiw and S. Templeton, *Topologically Massive Gauge Theories*, Annals. Phys. **140** (1982) 372 [Erratum-ibid. **185**, 406.1988 APNYA,281,409 (1988 APNYA,281,409-449.2000)].

[36] A. J. Niemi and G. W. Semenoff, *Axial Anomaly Induced Fermion Fractionization and Effective Gauge Theory Actions in Odd Dimensional Space-Times*, Phys. Rev. Lett. **51** (1983) 2077.

[37] A. N. Redlich, *Parity Violation and Gauge Noninvariance of the Effective Gauge Field Action in Three Dimensions*, Phys. Rev. **D29** (1984) 2366-2374.

[38] S. R. Coleman and B. Hill, *No More Corrections to the Topological Mass Term in* QED_3, Phys. Lett. **B159** (1985) 184-188.

[39] G. Dunne, *Aspects of Chern-Simons Theory*, Les Houches (1998), `hep-th/9902115`.

[40] A. B. Burd and J. D. Barrow, *Inflationary Models with Exponential Potentials*, Nucl. Phys. **B308** (1988) 929.

[41] S. Kachru, M. Shulz and E. Silverstein, *Self-Tuning flat Domain walls in 5d Gravity and String Theory*, Phys. Rev. **D62** (2000) 045021, `hep-th/0001206`.

[42] A. M. Ghezelbash, *Cosmological Solutions on Atiyah-Hitchin Space in Five Dimensional Einstein-Maxwell-Chern-Simons Theory*, Phys. Rev. **D81** (2010) 044027, `arXiv:1001.5066`.

[43] A. M. Ghezelbash, *Cosmological Solutions in Five Dimensional Minimal Supergravity*, Class. Quant. Grav. **27** (2010) 245025, `arXiv:1011.1433`.

[44] J. P. S. Lemos and V. T. Zanchin, *Rotating Charged Black String and Three-Dimensional Black Holes*, Phys. Rev. **D54** (1996) 3840-3853, `hep-th/9511188`.

[45] A. Einstein and N. Rosen, *On Gravitational Waves*, J.Franklin Inst. **223** (1937) 43-54.

[46] S. Chandrasekhar, *Cylindrical Waves in General Relativity*, Proc. Roy. Soc. Lond. **A408** (1986) 209-232.

[47] A. Ashtekar and M. Pierri, *Probing Quantum Gravity Throught Exactly Soluble MidiSuperspaces 1*, J. Math. Phys. **37** (1996) 6250-6270, `gr-qc/9606085`.

[48] J. Fernando Barbero, G. A. Mena Marugán, E. J. S. Villaseñor, *Microcausality and Quantum Cylindrical Gravitational Waves*, Phys. Rev. **D67** (2003) 124006, `gr-qc/0304047`.

[49] J. Fernando Barbero, I. Garay, E. J. S. Villaseñor, *Exact Quantization of Einstein-Rosen Waves Coupled to mass-less Scalar Matter*, Phys. Rev. Lett. **95** (2005) 050501, `gr-qc/0506093`.

[50] P. Castelo Ferreira, *Electro-Magnetic Space-Time Duality for* $2+1D$ *Stationary Classical Solutions*, Scripta-Ingenia **8** (2017) 3-8, `hep-th/0506244`.

[51] C. W. Misner, K. S. Thorne and J. A. Wheeler, *Gravitation*, W. H. Freeman and Company.

[52] R. Arnowitt, S. Deser and C. W. Misner, *The Dynamics of General Relativity* (1962) 227-265.

[53] S. Carlip, *Quantum Gravity in* $2+1$ *Dimensions*, 2003 - Cambridge University Press.

[54] S. Deser, M. Henneaux and C. Teitelboim, *Electric-Magnetic Black Hole Duality*, `hep-th/9607182`.

[55] S. Deser *Black Hole Electromagnetic Duality*, `hep-th/9701157`.

[56] S. Deser, A. Gomberoff, M. Henneaux and C. Teitelboim, *Duality, Self-Duality, Sources and Charge Quantization in Abelian* N*-Form Theories*, `hep-th/9702184`.

[57] J. D. Jackson, *Classical Electrodynamics*, 2^{nd} Edition, John Wiley & Sons, 1975.

[58] D. I. Olive, *Exact Electromagnetic Duality*, Nucl. Phys. Proc. Suppl. **45A** (1996) 88-102; Nucl. Phys. Proc. Suppl. **46** (1996) 1-15, `hep-th/9508089`.

[59] T. Regge and C. Teitelboim, *Role of Surface Integrals in the Hamiltonian Formulation of General Relativity*, Annals. Phys. 88 (1974) 286.

[60] P. C. R. Cardoso de Mello, S. Carneiro e M. C. Nemes, Phys. Lett. **B384** 197, `hep-th/9609218`.

[61] P. Castelo Ferreira, *Explicit Actions for Electromagnetism with Two Gauge Fields with Only one Electric and one Magnetic Physical Fields*, J. Math. Phys. **47** (2006) 072902, `hep-th/0510063`.

[62] P. Castelo Ferreira, *A Pseudo-Photon in Non-Trivial Background Fields*, Phys. Lett. **B651** 74-78, `hep-ph/0609239`.

[63] P. Castelo Ferreira, $U_e(1) \times U_g(1)$ *actions in* $2+1$*-dimensions: Full vectorial electric and magnetic fields*, Europhys. Lett. **79** (2007) 20004, `hep-th/0703193`.

Biodegradable materials from coconut products

by Vidhura Mahendra

Centre for Rapid and Sustainable Product Development
Polytechnic Institute of Leiria
Author email: vidhura.mahendra@ipleiria.pt

Abstract In this brief article we will be looking in to touch some of the significant uses of the coconut products with respect to its biodegradable aspect in addition to its worthiness as a wholesome food.

Biodegradation We hear the term *biodegradation* or *biodegradability* more often now than ever for all the reasons you can imagine. The term often used in tandem with recycling although the latter does not directly involve biological mechanism for the degradation. Biodegradation is the degradation mechanism related to living materials involved with microorganisms such as bacteria over a certain period of time. These materials are then used as growth materials for fresh life forms, biogenesis, e.g. plants, animals etc. On the other hand recycling is the reuse of produced materials individually or collectively by way of processing to different components, which may or may not be degradable. However, to our interest we will explore the biodegradability or biodegradable materials produced with related to coconut or coco as it is referred to as opposed to recycling or recyclable materials.

Coconut Coconuts are known for their great resourcefulness, as evidenced by many traditional exploits, ranging from food to cosmetics and lately as a potential energy generating mode. They form a regular part of the diets of many people in the tropics and subtropics, Sri Lanka, India, Philippine, Indonesia and Thailand in particular. Coconuts are distinct from other fruits for their large quantity of water which can be consumed as a refresher and sometimes given as a supplement that contains essential electrolytes. When mature, they can be used as seed nuts or processed to furnish oil from the kernel, charcoal from the hard shell, and coir from the fibrous husk. In Sanskrit it is called as kalpa vriksha ("the tree which provides all the necessities of life"). In the Malay language it is called pokok seribu guna("the tree of a thousand uses"). In the Philippines, the coconut is commonly called the "tree of life"In Sri Lanka there is an established coconut-based industry largely for the consumption of its milk and oil as food, a Sri Lankan food dish without them is almost inconceivable. The coconut tree is sometimes attributed to the ‘tree of the heaven’ (‘Surathura’ in Sinhala language), as the whole coconut tree is used for many different applications and none is being spared as waste material in daily life. Figure 1 shows coconuts grown in a tree from Sri Lanka.

Fig. 1 — Coconuts frown in a tree in Sri Lanka

The oil and milk are commonly used in cooking and frying, as well as in soaps and cosmetics. The husks and leaves can be used as material to make a variety of products for furnishing and decorating. The coconut also has cultural and religious significance in certain societies, particularly in India where it is used in Hindu rituals [1]. Vinegar and alcohol manufacturing are also some of the essentials products as part of coconut derivatives.

Fig. 2 — A bottle of coconut vinegar [1]

[1]picture credit http://indiatoday.intoday.in/story/7-reasons-to-move-on-from-acv-to-coconut-vinegar-it-has-got-coconut-water-apple-cider-vinegar/1/525565.html

Table 1 — Nutritional value per 100 g (3.5 oz)

Energy	354 kcal (1480 kJ)
Carbohydrates	15.23 g
Sugars	6.23 g
Dietary fiber	9.0 g
Fat	33.49 g
Saturated	29.698 g
Monounsaturated	1.425 g
Polyunsaturated	0.366 g
Protein	3.33 g
Tryptophan	0.039 g
Threonine	0.121 g
Isoleucine	0.131 g
Leucine	0.247 g
Lysine	0.147 g
Methionine	0.062 g
Cystine	0.066 g
Phenylalanine	0.169 g
Tyrosine	0.103 g
Valine	0.202 g
Arginine	0.546 g
Histidine	0.077 g
Alanine	0.170 g
Aspartic acid	0.325 g
Glutamic acid	0.761 g
Glycine	0.158 g
Proline	0.138 g
Serine	0.172 g
Vitamins	
Thiamine (B1)	(6%) 0.066 mg
Riboflavin (B2)	(2%) 0.020 mg
Niacin (B3)	(4%) 0.540 mg
Pantothenic acid (B5)	(6%) 0.300 mg
Vitamin B6	(4%) 0.054 mg
Folate (B9)	(7%) 26e−3 mg
Vitamin C	(4%) 3.3 mg
Vitamin E	(2%) 0.24 mg
Vitamin K	(0%) 0.2e−3 mg
Minerals	
Calcium	(1%) 14 mg
Iron	(19%) 2.43 mg
Magnesium	(9%) 32 mg
Manganese	(71%) 1.500 mg
Phosphorus	(16%) 113 mg
Potassium	(8%) 356 mg
Sodium	(1%) 20 mg
Zinc	(12%) 1.10 mg
Other constituents	
Water	46.99 g

The nutritional content of the coconut kernel is shown in the table 1 suggests the immense value of the coconut kernel as a food [2].

Historical aspect of coconut In the bygone era some of the tropical countries, Sri Lanka in particular whose history intertwined with coconut fibre or coir products especially in the rural areas for the local market such as floor mats, doormats, brushes, ropes and mattresses. This is largely due to its mass availability thus the cost effectiveness. However, with the dawn of the open economic policies in such countries leading to globalisation subsequent to 1970s the end products based on coir have been gradually replaced by the cheap alternative yet mass production of petroleum based product commonly known as plastics. The plastic find was revolutionary yet with some dire consequences, notably the non-degradation of its processed object. The global impact on non-degradation of plastics has been alarming in modern times, hence the lookout for plastic alternatives, in the form of biodegradation. In other words the world is looking for damage limitations. As a blessing in disguise we are deemed to reconsider what our ancestors did before with a hint of science and technology smeared with engineering over it.

Advances in coconut products As coir consists of considerable strength that can be applied by itself or reinforced with other suitable materials. Scientists have shown various properties of coir, the mechanical properties and degradation of the fibre over time subsequent to different processing techniques, but we do not intend to investigate such techniques in detail as that would be of academic relevance. However, as we embrace science and technological development in the contemporary world, the other significant uses of the coconut have been explored and discussed too, especially for advanced applications as a potential biodegradable material. In such matters the coir of the coconut becomes a pivotal part of the ongoing research and development across the board both academically and commercially. As with research studies pointing positive health impacts related to coconut milk and oil it is also noteworthy to look at some of the brighter side of the coir products as a separate entity, an emerging green product development.

It would be a tough task to throw away any of the components that derive from coco due to its versatility as discussed before. However, all these components have to be dissected carefully in order to produce a material that is of significance. In terms of coir, this can be processed to fabricate many commodities with considerable strength and biodegradable factor.

Products of coir In some parts of the world the coconut coir logs (Figure 3) are used as a biodegradable erosion control option for hills, banks, shorelines, and other erosion prone areas.

Fig. 3 — Coconut coir logs [2]

The logs can be effectively used in restoration projects, stabilization areas, and construction job sites due to its moisture retaining properties. Ease of Installation, providing nutrients to surrounding areas, allowing for deep rooting of plants, helping to build into existing contours, requiring no chemical treatment, high air and water permeability, environmentally friendly, safe for surrounding wildlife, biodegrades over 2-5 years, effectively holding seeds and saplings in place are some of the benefits of these coir logs. In addition to finely made coir logs, mats, blocks and wattles can also be named as some of the products for erosion control purpose.

Biodegradable chairs and flower pots Coir can be made as different layers to blend with latex and to stack them onto each other for desired stiffness and fibre density. Dutch designer Jorrit Taekema has fabricated a biodegradable chair (See Figure 4) out of such layered coco fibres. It appears as if a proper sofa type chair though its durability, strength and sustainability have not been evaluated. Moreover, biodegradable flower pots are widely made for the gardens.

Biodegradable erosion control blanket 100% chemically untreated coir fibre blankets can be fabricated. They are woven in different threads and sizes. Since they are of high amount of lignin (cellulose containing), coconut fibres are decomposition resistant. They last far more than other blankets and are tear resistant. For all these reasons, when the germinating period of a plant lasts for more than a vegetative season, Coir fibre blankets are used in bioengineering methods for superficial stabilization. These blankets are used in slope and bank covering, slopes with erosion control problems and complete biodegradation is estimated within five years.

Fig. 4 — A biodegradable coconut fibre chair designed by Jorrit Taekema [3]

Decorative pots and hanging bowls Appropriate decorative pots and hanging bowls can also be created using coir and latex with better air circulation, water absorption with high water and fertilizer retention properties. Weed prevention disks & mats can be made to provide continuous soil cover to retain moisture and prevent soil erosion while preventing weed growth.

Scope of coir products In an ideal world there could be plenty of limitations around us but in a world with many creators and innovators the limit for the coir products is endless. As with the advancement of science and technology we can expect more fascinating objects to materialise upon us that would not destroy and clatter our beautiful world but eventually leave just like us one day.

Referências

[1] Coconut – fruit of lustre in Indian culture by Vimal Patil, http://www.esamskriti.com/essay-chapters/Coconut- -Fruit-of-Lustre-in-Indian-Culture-1.aspx

[2] The data obtained from the National nutrient database for standard reference release 28, United States department of Agriculture agricultural research service. https://ndb.nal.usda.gov/ndb/foods/show/3656?fgcd=

[2] Picture credit `http://ecesupplies.com.au/?page_id=250`

[3] Picture credit `http://jorrittaekema.com/DESIGN/JORRIT_TAEKEMA_-_PRODUCTS.html`